ARF-2068-5

ARF

ARMOUR RESEARCH FOUNDATION OF ILLINOIS INSTITUTE OF TECHNOLOGY

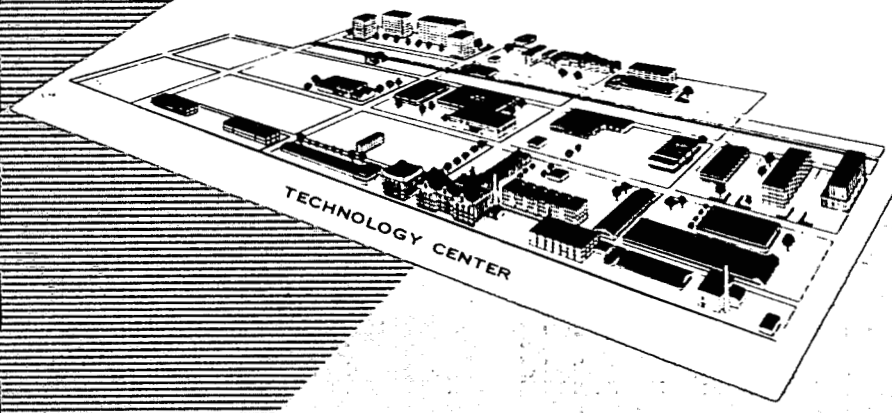

ARF Project B 068
Contract No. AT(11-1)-315

THE SYSTEM ZIRCONIUM-IRON-TIN

Report No. 5, Summary

RESEARCH FOR INDUSTRY

DISCLAIMER

ARMOUR RESEARCH FOUNDATION
of
ILLINOIS INSTITUTE OF TECHNOLOGY
Technology Center
Chicago 16, Illinois

AEC Research and Development Report

ARF-2068-5
Project No. B 068
Contract No. AT(11-1)-315

THE SYSTEM ZIRCONIUM-IRON-TIN

Report No. 5, Summary
July 1, 1957 - June 30, 1958

Submitted to:

United States Atomic Energy Commission
Washington 25, D.C.

by

Lee E. Tanner
Metals Research Department

July 29, 1958

DISTRIBUTION LIST

Ames Laboratory
P.O. Box 14A, Station A
Ames, Iowa
Attention Dr. F. H. Spedding — 1

Argonne National Laboratory
P.O. Box 299
Lemont, Illinois
Attention Dr. Hoylande D. Young — 4

Atomics International
Div. North American Aviation Inc.
P.O. Box 309
Canoga Park, California
Attention Dr. Chauncey Starr — 1

Battelle Memorial Institute
505 King Avenue
Columbus 1, Ohio
Attention Dr. H. W. Russell — 1

Brookhaven National Laboratory
Technical Information Division
Documents Group
Upton, L.I., New York — 3

Carbide & Carbon Chemicals Div.
K-25 Records Department
P.O. Box P
Oak Ridge, Tennessee — 2

Dow Chemical Company
Rocky Flats Plant
P.O. Box 2131
Denver, Colorado — 1

E. I. DuPont deNemours & Co.
Explosives Department
Atomic Energy Division
Wilmington 98, Delaware
Attention Document Custodian — 2

General Electric Company
ANP Division
P.O. Box 132
Cincinnati 15, Ohio
Attention Director, Materials Res. — 1

General Electric Company
Technical Information
P.O. Box 100
Richland, Washington
Attention Miss M. G. Freidank — 2

Institute for the Study of Metals
University of Chicago
Chicago 37, Illinois
Attention Dr. Cyril S. Smith — 1

Knolls Atomic Power Laboratory
P.O. Box 1072
Schenectady, New York
Attention Document Librarian — 3

Los Alamos Scientific Laboratory
P.O. Box 1663
Los Alamos, New Mexico
Attention Report Librarian — 2

Mound Laboratory
P.O. Box 32
Miamisburg, Ohio
Attention Central Files — 2

National Advisory Committee
for Aeronautics
Lewis Flight Propulsion Laboratory
21000 Brookpark Road
Cleveland 11, Ohio
Attention Director, Materials Res. — 1

National Bureau of Standards
Connecticut Ave. & Van Ness St., N.W.
Washington 25, D.C.
Attention Dr. L. S. Taylor — 2

Nuclear Metals, Inc.
155 Massachusetts Avenue
Cambridge 39, Massachusetts
Attention Dr. A. R. Kaufmann — 1

Oak Ridge National Laboratory
P.O. Box P
Oak Ridge, Tennessee
Attention Central Files — 4

DISTRIBUTION LIST (continued)

Sandia Corporation — 1
Sandia Base
Document Division
Albuquerque, New Mexico

Sylvania Electric Products Inc. — 2
Atomic Energy Division
P.O. Box 6
Bayside, L.I., New York
Attention Document Custodian

U.S. Atomic Energy Commission — 2
1901 Constitution Ave., N.W.
Washington 25, D.C.
Attention Technical Library

U.S. Atomic Energy Commission — 1
Division of Research
1901 Constitution Ave., N.W.
Washington 25, D.C.
Attention Chief, Metallurgy
& Materials Branch

U.S. Atomic Energy Commission — 1
1901 Constitution Ave., N.W.
Washington 25, D.C.
Attention Chief, Patent Branch

U.S. Atomic Energy Commission — 1
Hanford Operations Office
P.O. Box 550
Richland, Washington

U.S. Atomic Energy Commission — 1
Idaho Operations Office
P.O. Box 1221
Idaho Falls, Idaho
Attention Technical Library

U.S. Atomic Energy Commission — 3
New York Operations Office
70 Columbus Avenue
New York 23, New York
Attention Div. of Technical Information

U.S. Atomic Energy Commission — 1
Oak Ridge Operations Office
P.O. Box E
Oak Ridge, Tennessee
Attention Dr. H. M. Roth

Dr. J. B. Johnson, Chief — 1
Metallurgical Group, WCRR
Wright-Patterson Air Force Base
Ohio

U.S. Atomic Energy Commission — 1
Schenectady Operations Office
P.O. Box 1069
Schenectady, New York
Attention Librarian

U.S. Department of the Navy — 1
Bureau of Ships, Code 490
Washington 25, D.C.

U.S. Department of the Navy — 1
Office of Naval Research, Code 423
Washington 25, D.C.

U.S. Naval Research Laboratory — 1
Washington 25, D.C.
Attention Librarian

U.S. Department of the Army — 1
Office of Ordnance Research
Box CM, Duke Station
Durham, North Carolina
Attention Dr. Peter Kosting

U.S. Department of the Air Force — 1
Office of Scientific Research
Baltimore, Maryland
Attention Mr. C. Yost

University of California — 3
Radiation Laboratory
Information Division
Room 128, Building 50
Berkeley 4, California
Attention Dr. R. K. Wakerling

University of California — 1
Radiation Laboratory
P.O. Box 808
Livermore, California
Attention Librarian

DISTRIBUTION LIST (continued)

U.S. Atomic Energy Commission — 15
Technical Information Service
P.O. Box 62
Oak Ridge, Tennessee

Westinghouse Electric Corporation — 2
Atomic Power Division
P.O. Box 1468, Bettis Plant
Pittsburgh 30, Pennsylvania
Attention Librarian

Westinghouse Electric Corporation — 1
Bettis Atomic Power Division
P.O. Box 1468
Pittsburgh 30, Pennsylvania
Attention Dr. D. E. Thomas
AlW Metallurgy Section

Attention Dr. K. M. Goldman — 1

Attention Dr. J. Hino — 1

Attention Mr. R. H. Fillnow — 1

Attention Mr. F. L. Shubert — 1

Oak Ridge National Laboratory — 1
P.O. Box X
Oak Ridge, Tennessee
Attention Dr. M. L. Picklesimer
Metallurgy Division

THE SYSTEM ZIRCONIUM-IRON-TIN

ABSTRACT

The zirconium-iron-tin system was investigated up to the first compound in each binary system ($ZrFe_2$ and Zr_4Sn) between the temperatures 500° and 1100°C. A careful study of the solubility of iron and tin in alpha-zirconium was also made between the temperatures 200° and 800°C. The alloys were prepared from "Grade 1" iodide zirconium (as received and electron bombardment melted) and high purity iron and tin by nonconsumable-electrode arc melting techniques under an inert atmosphere. Ingots were homogenized, cold worked when possible, cut or broken into small specimens, and given equilibration anneals at the prescribed temperatures.

Metallographic examination of the heat treated and quenched samples was the main method of investigation. X-ray diffraction and magnetic susceptibility techniques were also employed. The results of this program are summarized in 12 partial isothermal sections.

The phase relations determined in last year's program were confirmed, and phase boundaries were adjusted to their proper positions. The important features of the system are as follows:

(1) There is little solubility for tin in the compound $ZrFe_2$. The single-phase field is believed to exist in the vicinity of 55w/o Fe.

(2) The compound theta appears to be a continuous phase originating at the binary compound (Zr_4Sn) and dissolving up to about 7.5w/o Fe while maintaining a constant tin composition of the order of 24.5w/o.

(3) A four-phase ternary eutectic ($L \rightleftharpoons \beta + \theta + ZrFe_2$) occurs between 930° and 935°C.

(4) It is likely that a four-phase ternary peritectoid ($\beta + \theta \rightleftharpoons \alpha + ZrFe_2$) occurs at a temperature just above the binary zirconium-iron eutectoid (which takes place between 790° and 800°C). A four-phase ternary eutectoid ($\beta \rightleftharpoons \alpha + \theta + ZrFe_2$) taking place just above the zirconium-iron eutectoid remains an alternate possibility.

(5) The solubility limit of alpha-zirconium was found to be extremely low in the presence of iron, falling below the most dilute binary iron and ternary alloys prepared at temperatures of 600°C and lower.

TABLE OF CONTENTS

LIST OF ILLUSTRATIONS

LIST OF ILLUSTRATIONS (continued)

LIST OF TABLES

THE SYSTEM ZIRCONIUM-IRON-TIN

I. INTRODUCTION

In accordance with Contract AT(11-1)-315 entitled "A Study of the Mechanisms of Heat Treatment of Zirconium-Base Alloys," investigation of the zirconium-rich portion of the zirconium-iron-tin system was carried on for the second year. This work was part of the supplement to the contract entitled "Phase Diagram Studies."

The first year's work produced partial isothermal sections between the temperatures 500° and 1100°C inclusive (in 100-degree intervals), up to the first compound in the binary zirconium-iron and zirconium-tin systems ($ZrFe_2$ and Zr_4Sn, respectively).[1] This program was extended to the study of the solubility of iron and tin in alpha-zirconium at temperatures between 200° and 800°C. In addition, the phase boundaries determined in the previous year's work were checked carefully.

Small ingots of the alloys were prepared by arc melting the highest purity materials available. Following proper pretreatment the alloys were annealed at 50-degree intervals between 200° and 500°C and 100-degree intervals between 500° and 1100°C. Heat treatments of certain alloys at other temperatures were used to establish critical phase transformations. Metallographic examination of the structures quenched from the various temperatures was the major mode of investigation. Also incorporated were X-ray diffraction techniques and magnetic susceptibility measurements.

II. MATERIALS

A. Zirconium

Zirconium crystal bar, produced by the decomposition of a volatile iodide, was used for all these studies. High purity, Grade 1, hafnium-free

material was supplied by the AEC. The manufacturer's analysis appears in Table I. The zirconium used for the alpha solubility studies was electron bombardment melted by Temescal Metallurgical Corporation. This was done in an effort to lower the iron level as well as to further purify the material through the use of a high vacuum.

B. Preparation of Zirconium Melting Stock

The zirconium crystal bar, as-received, was coated with corrosion product from autoclave tests by which its grade designation is determined. The bars were sand-blasted lightly, pickled for 1 minute in a 20% HNO_3-5% HF aqueous solution, rinsed in water and acetone, and dried. The bars were rolled to about 1/32 in. strip. The strip was cut into 10 in. lengths and pickled and rinsed again. The material was sheared to approximately 1/4 in. squares, cleaned with acetone and stored. The electron bombardment melted ingots were handled in an identical manner.

C. Iron and Tin

High-purity, gas-free iron was supplied by National Research Corporation. High-purity tin was received from the Vulcan Detinning Company. Typical analyses of these materials appear in Table II.

D. Preparation of Iron and Tin Melting Stock

The iron bar was cleaned by taking small lathe cuts. The rod was sliced into 3/4 in. thick pieces and cold-rolled to 0.050 in. sheet. The sheet was sand-blasted lightly, vigorously rinsed in acetone, dried, and bottled for storage in mineral oil to prevent oxidation prior to arc melting.

Hemispherical ingots of tin were cut in sections, cold-rolled to approximately 1/32 in. sheet strip, sheared, cleaned in acetone, and bottled for storage.

TABLE I

ANALYSIS OF GRADE 1 ZIRCONIUM CRYSTAL BAR

Element	Concentration, ppm
Al	<35
C	33
Cu	<25
Fe	27
Mg	<10
Ti	<25

TABLE II

LOT ANALYSES OF IRON AND TIN

Element	Concentration, w/o
Iron	
N	<0.001
O	<0.02
H	<0.005
Al	<0.001
C	<0.005
Cr	<0.001
Co	<0.001
Cu	<0.001
Mn	<0.001
Mo	<0.001
Ni	<0.001
Si	<0.001
Sn	<0.01
Ti	<0.001
W	<0.001
Tin	
Fe	0.0020
Sb	0.0002
Pb	nil
Cu	nil

III. EQUIPMENT AND EXPERIMENTAL PROCEDURES

A. Arc Melting of Alloys

A nonconsumable-electrode arc melting furnace was used to prepare the alloys. This furnace has been widely used for the preparation of titanium, vanadium and zirconium alloys. A water-cooled copper crucible and a tungsten-tipped electrode were employed. The material is placed in the crucible and rapidly melted under a protective atmosphere of helium or argon gas by striking the arc on a tungsten stud and then transferring the arc to the charge material. A drawing of the furnace and a description of general melting techniques have been published.[2] Control melts of unalloyed zirconium were prepared and checked for hardness and microstructure thoughout the melting program.

The dilute alloys for the alpha solubility studies were in the form of 10-gram button ingots using the electron bombardment melted iodide zirconium. All others were based on iodide crystal bar and weighed 15 grams.

B. Heat Treatment

Prior to regular isothermal equilibration annealing treatments, the alloys were given a homogenization pretreatment. Cold pressing was employed to speed the approach to equilibrium of alloy compositions which were ductile (<10w/o Fe and <10w/o Sn).

Preparation for equilibration heat treatments consisted of cold pressing and rolling ductile alloys to approximately 3/16 in. thickness and then sawing the sheet into small samples. The brittle compositions were broken with hammer and chisel. The specimens were sealed in Vycor bulbs. A partial pressure of argon was admitted to prevent the bulbs from collapsing during anneals at temperatures above 900°C. For lower temperature anneals, bulbs were completely evacuated. Specimens for treatment above 900°C were individually

wrapped in molybdenum sheet for protection in the event of incipient melting of some compositions. When phase fields where liquid was present were specifically checked, the alloys were encapsulated in individual Vycor bulbs. Quenching was accomplished by breaking the bulbs under cold water or iced brine.

Resistance-type, porcelain tube furnaces, whose control was within ±3°C, were employed. Temperatures were measured twice daily with a calibrated thermocouple for long-time anneals, and at more frequent intervals for short-time anneals.

C. Metallographic Techniques

The first step in preparing samples for metallographic examination was to mount them in Bakelite. A belt sander employing 120-grit, silicon carbide abrasive rough polished a preliminary flat surface. This was followed by the use of silicon carbide papers of grit Nos. 240, 320, 400 and 600. An alternate procedure incorporated a Lapmaster unit using Lapmaster 1900 lapping compound plus several passes on No. 600 paper. The final polishing operation involved two steps: polishing on airplane cloth impregnated with diamond paste in a kerosene vehicle, then on silk impregnated with "Linde B" synthetic sapphire, distilled water being the vehicle. The etchant employed on most of the alloys was a solution of 20% HF and 20% HNO_3 in glycerine which was swabbed on the polished surface. Etching times ranged between 1 and 30 seconds. The dilute alloys required careful etching with the above solution (or one made dilute by addition of glycerine) for periods of 1 to 10 seconds followed by a water rinse. Subsequently, the specimens were swabbed rapidly by a solution of 50% H_2O_2, 45% HNO_3, and 5% HF.

D. X-Ray Equipment and Techniques

A 14-centimeter Debye-Scherrer powder camera and nickel-filtered copper radiation served for all X-ray work on this system. Minus 320 mesh

powders were prepared by crushing heat-treated samples and were examined without stress-relief annealing.

E. Analytical Procedures

1. Iron

The alloy sample was dissolved in a mixture of HCl and HF. Then an aliquot was taken and the iron reduced with $H_2NOH \cdot HCl$. The sample was buffered with $NaC_2H_3O_2$ and the characteristic ferrous orthophenanthroline color developed by the addition of orthophenanthroline. Following the adjustment of the sample to a standard volume, the optical density of the color complex and concentration was determined.

2. Tin

The zirconium sample is dissolved in a mixture of dilute HBF_4-H_2SO_4. The solution is diluted and HCl is added. Sn^{IV} is reduced to Sn^{II} with iron powder. Stannous tin is titrated with a standard iodine or iodate solution to the starch-iodine end point.(3)

3. Nitrogen

The sample is placed in a beaker containing 10 ml of 1:1 H_2SO_4. Heat is applied until a reaction becomes apparent. The solution of the sample is allowed to proceed at its own rate on a low hot plate. Then 10 ml of water and one drop of HF are added to the cool solution, and dissolution is completed. The solution is made strongly basic with NaOH, and the ammonia is distilled off into a 4% boric acid solution and titrated with standard acid.

4. Oxygen and Hydrogen

National Research Corporation vacuum fusion apparatus was employed for these analyses. Standard procedures using a platinum bath were followed.

F. Magnetic Susceptibility

Of the two compounds present in this portion of the zirconium-iron-tin system, $ZrFe_2$ was found to be ferromagnetic while theta (the ternary modification of Zr_4Sn) is nonferromagnetic. Therefore, magnetic susceptibility measurements were considered as a possible method for determining the presence or absence of $ZrFe_2$ in dilute alloys having a nonferromagnetic matrix of alpha-zirconium. The susceptibility apparatus used was of the Curie[4] type and incorporated an analytic balance to measure the magnetic force on samples suspended in the field of an electromagnet. The system was calibrated using a standard sample of palladium.

IV. RESULTS AND DISCUSSION

A. Purification of Iodide Zirconium

Three ingots were prepared by the high vacuum, electron bombardment melting of iodide crystal bar. The ingot with the lowest hardness (VPH 69) and the cleanest microstructure was used for preparation of dilute alloys. The main purpose of using this melting technique was to lower the existing iron level which depended on the higher vapor pressure of iron at the melting point of zirconium. However, spectrochemical analysis indicated the iron content remained essentially unchanged (of the order of 27 ppm).

The process had a remarkable effect on the microstructure as is seen when comparing the amount of precipitate in iodide crystal bar (Figure 1) with that found in electron bombardment melted stock (Figure 3). Arc melting both these materials produced an increase in precipitate as seen in Figures 2 and 4. Chemical analyses of these samples (Table III) indicates a small degree of impurity pickup with both types of melting. Only hydrogen is insoluble in alpha-zirconium at low temperatures, and the relative amount of precipitate in

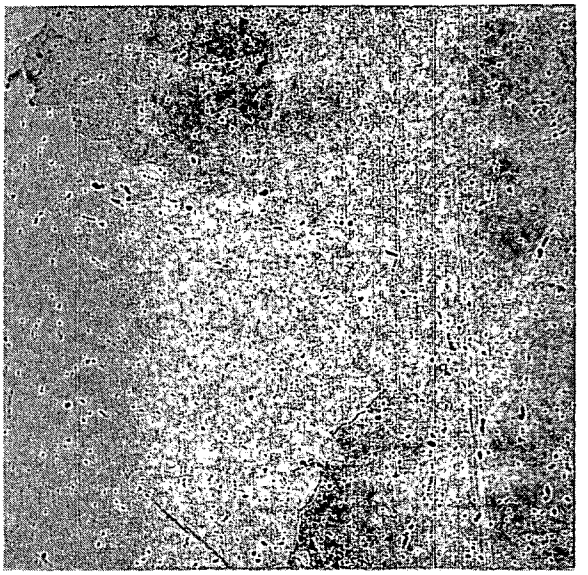

Neg. No. 16466 X 250

Fig. 1

Iodide zirconium crystal bar.

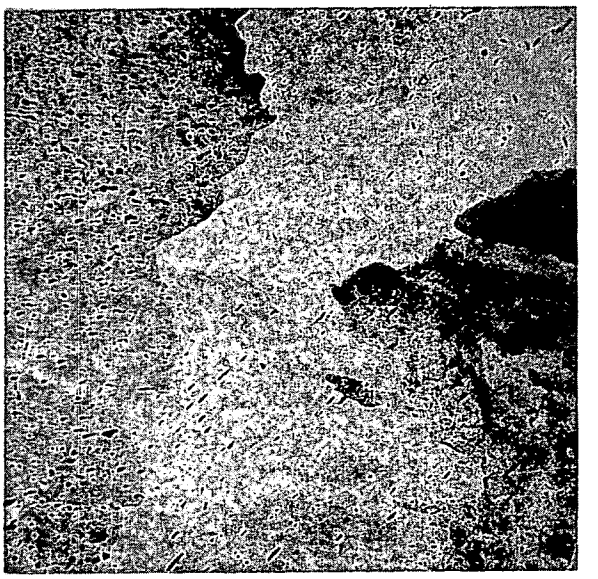

Neg. No. 16140 X 250

Fig. 2

Arc-melted iodide zirconium crystal bar.

Neg. No. 16138 X 250

Fig. 3

Electron bombardment melted iodide zirconium crystal bar.

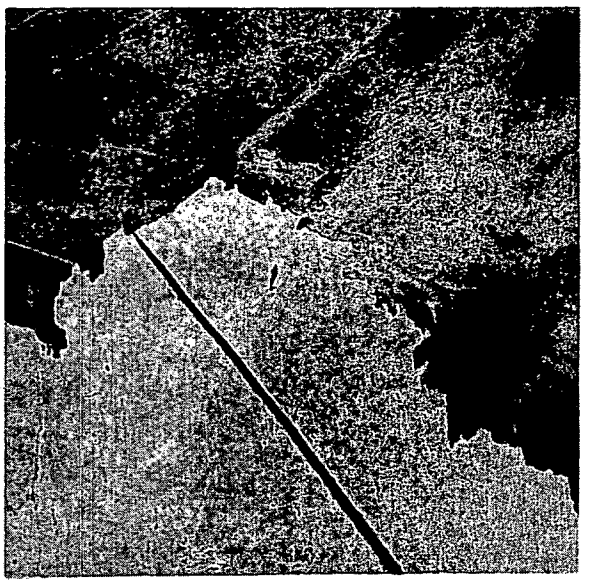

Neg. No. 16143 X 250

Fig. 4

Arc-melted, electron bombardment melted iodide zirconium crystal bar.

Etchant: 20% HF, 20% HNO_3 in glycerine.

TABLE III

ANALYSES FOR NITROGEN, OXYGEN AND HYDROGEN IN PURE ZIRCONIUM

Material	Nitrogen (w/o)	Oxygen (w/o)	Hydrogen (ppm)
Iodide crystal bar, as received	nil	0.0037	nil
Iodide crystal bar, arc melted	0.010	0.0092	30
Electron bombardment melted, as received	0.0009	0.019	4
Electron bombardment melted, arc melted	0.0024	0.020	10

Figures 2, 3 and 4 seems to correlate well with the relative hydrogen contents of the respective specimens. This solubility is quite high in the range of 800°C, but decreases drastically over a small temperature drop, making the suppression of hydride precipitation during cooling quite difficult. This could explain the presence of precipitate in varying amounts in all-alpha structures quenched from temperatures where hydrogen would be expected to be in solution. However, the large amount of precipitate in the unmelted crystal bar (Figure 1), where there is essentially no hydrogen present, is not consistent with this point of view.

Metallographically, hydride usually is found in the form of platelets as seen in Figure 2, but has been known to take on a round particle shape as well. The low solubility of iron in alpha points to the possibility of some of the precipitate being $ZrFe_2$. This will be discussed in a later section. It is felt, however, that until more conclusive evidence is obtained, the identification of the precipitate as hydride is the most sound.

B. Alloys

A series of 81 alloys based on iodide crystal bar were prepared to check the phase boundaries of the zirconium-iron-tin system. The nominal compositions are listed in Table IV. In addition, these compositions are plotted in Figure 5 which also includes the 94 alloys prepared for the previous year's program. Weight gains after melting were not encountered, and weight losses were negligibly small. In the past[1] it was found that there was good agreement between nominal and analyzed compositions. It was assumed that such agreement could be expected in all alloys. Therefore, chemical analyses were made only of alloys which appeared to delineate phase boundaries, or those which, for other reasons, required confirmation of composition.

TABLE IV

NOMINAL COMPOSITIONS OF ZIRCONIUM-IRON-TIN ALLOYS*

Alloy No.	Weight Per cent Iron	Tin	Alloy No.	Weight Per cent Iron	Tin
98	0.5	5.0	150	16.5	10.0
99	1.0	5.0	151	17.0	7.5
100	1.5	5.0	152	17.5	7.5
101	1.5	11.0	153	25.0	0.1
102	2.0	10.5	154	25.0	0.2
103	2.5	1.5	155	25.0	0.3
104	2.5	5.0	156	25.0	0.4
105	2.5	10.0	157	25.0	0.5
106	2.5	23.0	158	25.0	1.0
134	9.0	16.0	159	25.0	1.5
135	9.5	15.5	162	40.0	7.0
136	10.0	0.1	163	40.0	7.5
137	10.0	0.2	164	40.0	8.0
138	10.0	0.3	165	40.0	8.5
139	10.0	0.4	166	25.0	15.5
140	10.0	0.5	167	25.0	16.0
141	10.0	1.0	168	25.0	16.5
142	10.0	1.5	174	2.5	23.5
143	12.0	7.5	175	2.5	24.0
144	12.5	7.5	176	2.5	24.5
145	13.0	7.5	177	3.0	1.5
146	13.5	7.5	178	3.0	9.5
147	14.0	7.5	179	3.0	10.0
148	15.5	10.0			
149	16.0	10.0			

TABLE IV (continued)

Alloy No.	Weight Per cent Iron	Tin	Alloy No.	Weight Per cent Iron	Tin
180	3.5	1.5	200	8.5	16.5
181	3.5	9.0	201	6.5	15.0
182	3.5	10.0	202	15.0	10.0
183	4.0	1.5	203	17.0	10.0
184	4.0	8.5	204	17.5	10.0
185	4.0	10.0	205	5.5	6.0
187	4.5	8.0	206	5.0	6.5
188	4.5	10.0	210	47.0	
189	5.0	7.5	211	50.0	
190	5.5	7.0	212	55.0	
191	5.5	15.0	213	55.0	1.0
192	6.0	6.5	214	55.0	0.5
193	6.0	15.0	215	7.5	24.5
194	6.5	6.0	216		26.0
195	7.5	17.5			
196	7.5	21.0			
197	7.5	21.5			
198	7.5	22.0			
199	8.0	17.0			

* Based on iodide zirconium.

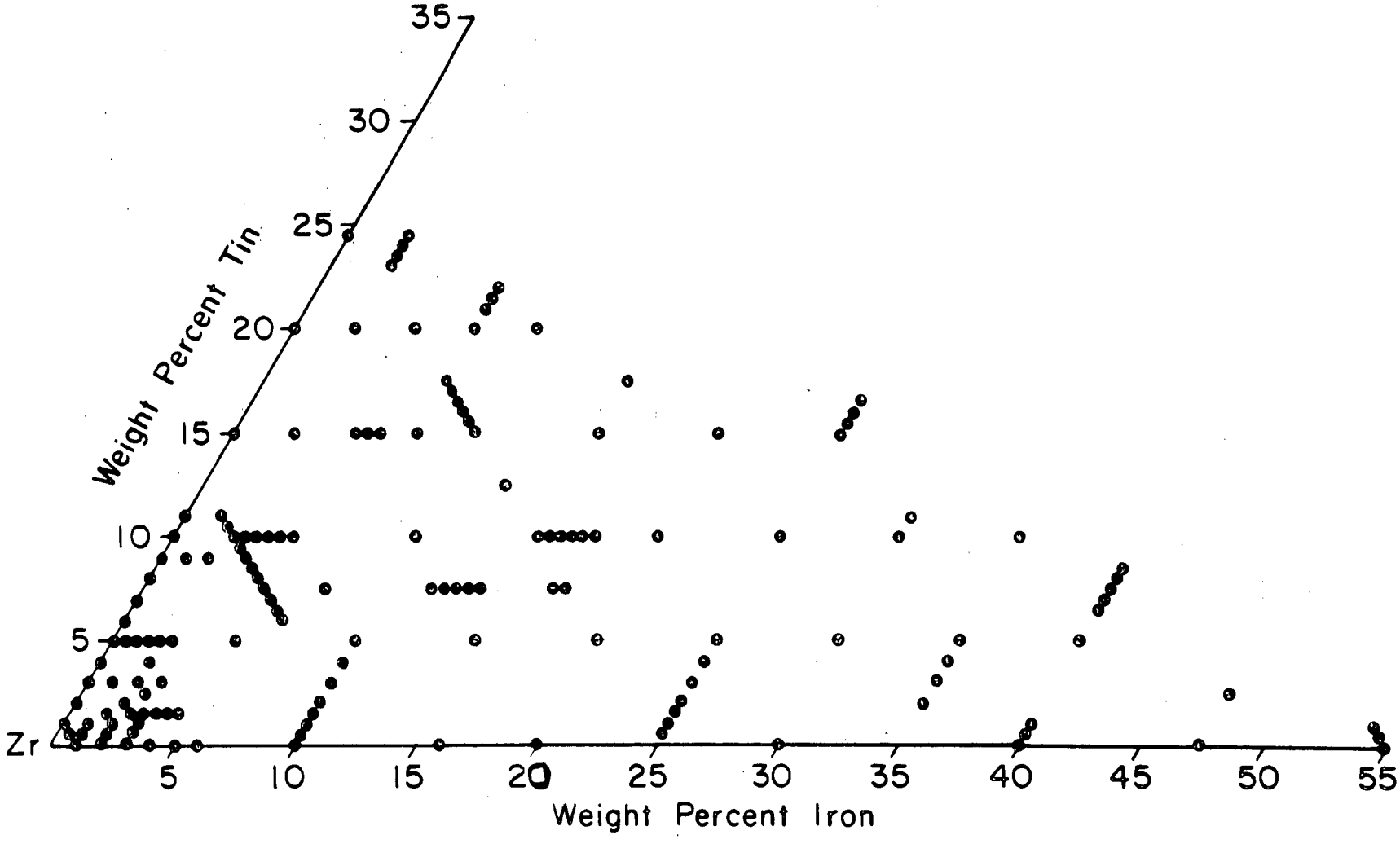

FIG. 5 - NOMINAL COMPOSITIONS OF ZIRCONIUM-IRON-TIN ALLOYS BASED ON IODIDE ZIRCONIUM

A series of 57 dilute alloys based on electron bombardment melted zirconium were prepared by arc melting for study of the alpha-phase boundary. The alloy constituents were added in the form of master alloys (0.45w/o Fe and 0.52w/o Sn). The nominal and analyzed compositions are presented in Table V and the analyzed compositions are plotted in Figure 6.

C. Heat Treatment

Homogenization pretreatments consisted of the following:

(1) Alloys based on iodide crystal bar were annealed at 850°C for 6 hours under a dynamic vacuum of <0.1 micron (1×10^{-4} mm of Hg) and air-cooled. This was followed by 29 hours at the same temperature sealed in evacuated Vycor bulbs and then water quenched.

(2) Dilute alloys based on electron bombardment melted zirconium were sealed in evacuated Vycor bulbs and annealed at 800°C for 50 hours followed by an iced-brine quench.

The schedule for isothermal equilibration anneals appears in Table VI. In general, annealing times were based on those used in last year's program.[1] Shorter periods at high temperatures, where considerable melting was expected, were necessary to prevent contamination by reaction of the liquid with the Vycor.

Duplicate samples of the dilute alloys were annealed at 400°, 450° and 500°C for 429 hours. These samples did not reach equilibrium in this period of time.

D. The Zirconium-Iron System

As was observed previously,[1] purity affects the phase relations in the zirconium-iron system. A critical study was made of this system using iodide material in order to obtain data consistent with the ternary system.

TABLE V

COMPOSITIONS OF ZIRCONIUM-IRON-TIN ALLOYS*

Alloy No.	Iron (w/o)		Tin (w/o)	
	Nominal	Analyzed	Nominal	Analyzed
300	0.500	0.450		
301			0.500	0.520
302	0.005	0.017		
303	0.010	0.012		
304	0.015	0.025		
305	0.020	0.028		
306			0.050	0.060
307			0.100	0.110
308			0.150	0.150
309			0.200	0.190
310			0.300	0.270
311			0.400	0.360
312			0.500	0.450
313			0.600	0.510
314			0.700	0.610
315			0.800	0.760
316	0.002	0.027	0.020	0.050
317	0.002	0.006	0.050	0.040
318	0.002	0.008	0.070	0.070
319	0.002	0.006	0.170	0.160
320	0.004	0.009	0.090	0.090
321	0.004	0.005	0.190	0.170
322	0.005	0.011	0.020	0.040
323	0.006	0.012	0.050	0.100
324	0.006	0.007	0.110	0.100
325	0.006	0.006	0.210	0.190
326	0.008	0.010	0.180	0.170
327	0.008	0.012	0.280	0.270
328	0.009	0.009	0.020	0.030
329	0.010		0.050	
330	0.010	0.015	0.250	0.245
331	0.010	0.017	0.400	0.379
332	0.011	0.013	0.110	0.107
333	0.012	0.015	0.270	0.251
334	0.012	0.027	0.420	0.400
335	0.013	0.014	0.130	0.170
336	0.014	0.019	0.050	0.054
337	0.014	0.015	0.440	0.420
338	0.015	0.018	0.150	0.130
339	0.016	0.019	0.460	0.433
340	0.017	0.017	0.170	0.150

TABLE V (continued)

Alloy No.	Iron (w/o)		Tin (w/o)	
	Nominal	Analyzed	Nominal	Analyzed
341	0.018	0.047	0.050	0.047
342	0.018	0.070	0.480	0.450
343	0.019	0.023	0.190	0.180
344	0.020	0.028	0.500	0.360
345	0.021	0.023	0.210	0.190
346	0.022	0.025	0.050	0.046
347	0.023	0.026	0.230	0.210
348	0.030	0.030		
349	0.040	0.050		
350	0.050	0.051		
351	0.060	0.066		
352	0.070	0.038		
353	0.080	0.070		
354	0.090	0.072		
355	0.100	0.090		
356	0.300	0.300		
357	0.500	0.460		
358	0.700	0.630		
359	1.000	0.980		

* Based on electron bombardment melted iodide zirconium.

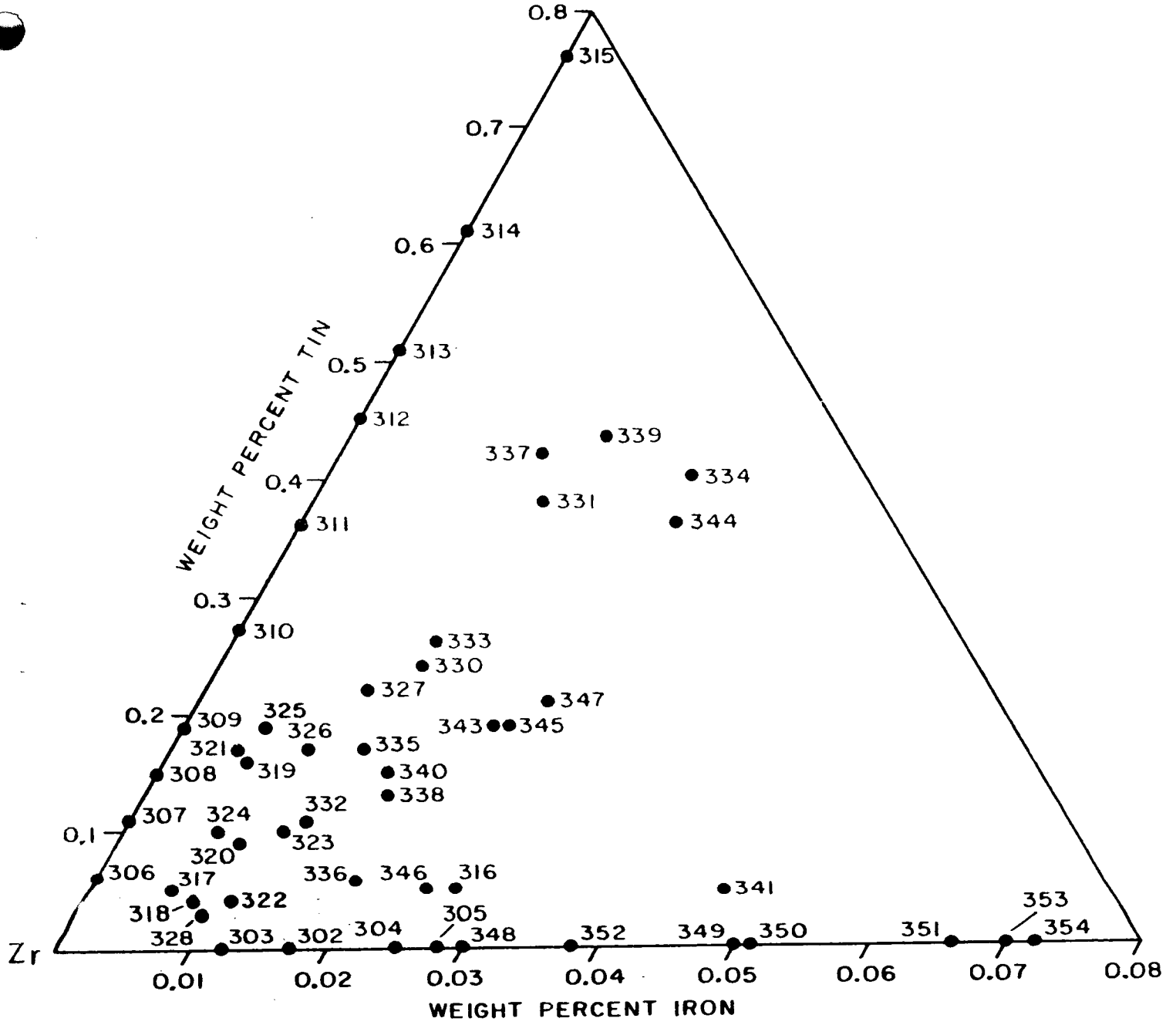

FIG. 6 - ANALYZED COMPOSITIONS OF ZIRCONIUM-IRON-TIN ALLOYS BASED ON ELECTRON BOMBARDMENT MELTED IODIDE ZIRCONIUM

TABLE VI

HEAT TREATMENTS OF ZIRCONIUM-IRON-TIN ALLOYS

Temp (°C)	Alloy No.	Time (hr)
1100	98-106,134,135,141-152,158,159,184,185,187-195,199-206[a]	5 to 30*
	136-141,153-157,162-168,174-183,196-198,210-215[a]	25
1000	98-106,134,135,141-152,158,159,184,185,187-195,199-206[a]	5 to 30*
	136-141,153-157,162-168,174-183,196-198,210-215[a]	40
950	143-147[a]	5 to 30*
940	143-147[a]	5 to 30*
935	143-147[a]	50
920	143-147[a]	50
900	98-106,134-159,162-168,174-185,187-206,210-215[a]	96
800	98-106,134-159,162-168,174-185,187-206,210-215[a]	264
790	(100,104),[a] (302-305,348-359)[b]	264
780	(100,104),[a] (302-305,348-359)[b]	264
775	(100,104),[a] (302-305,348-359)[b]	264
700	98-106,136-142,153-159,162-168,174-180,182,183,185,188,191, 193,196-198,201,202,215[a]	508
	302-354[b]	1203
600	98-106,136-142,153-159,162-168,174-180,182,183,185,188,191, 193,196-198,201,202,215[a]	744
	302-354[b]	1203
500	98-106,136-142,153-159,162-168,174-180,182,183,185,188,191, 193,196-198,201,202,215[a]	1008
	302-354[b]	429,1456
450	302-354[b]	429,1600
400	302-354[b]	429,1600

TABLE VI (continued)

Temp (°C)	Alloy No.	Time (hr)
350	302-354[b]	1768
300	302-354[b]	1768
250	302-354[b]	1800
200	302-354[b]	1800

* Time in minutes.

Homogenization pretreatments:

a 6 hours at 850°C under dynamic vacuum-air cool; 29 hours at 850°C-water quench.

b 50 hours at 800°C-iced brine quench.

The results of this work are summarized in the zirconium-rich portion of the diagram presented in Figure 7. All compositions were analyzed and are compared to the diagram presented by Hayes, Roberson and O'Brien[5] which was based on relatively impure sponge zirconium. They also reported carbon pickup during induction melting alloys in graphite crucibles as well as possible contamination due to hot working their alloys in air.

The following are the important features of the system based on iodide zirconium:

(1) The eutectic temperature is between 945° and 950°C and the maximum beta solubility is about 4.25w/o Fe at this temperature.

(2) The eutectoid temperature is between 790° and 800°C, and the eutectoid composition is of the order of 2.2w/o Fe. The maximum solubility of iron in alpha-zirconium is about 0.020w/o at the eutectoid temperature and drops to <0.010w/o at 700°C.

(3) There is some question as to whether or not the composition of the compound $ZrFe_2$ is the reported 47.5w/o. This will be discussed further in the following section.

E. The Zirconium-Iron-Tin System

1. The Partial Phase Diagram

In general, the phase relations reported in the last summary report[1] have been confirmed. By bracketing the phase boundaries with the new alloys it was possible to adjust them to their proper positions. The final results are presented in the form of 9 new partial isothermal sections for the temperatures 1100° through 500°C in 100-degree intervals (Figures 8 through 16) documented with data points based on nominal compositions. This sequence also includes expanded portions of the 900° and 800°C isotherms (Figures 11 and 13, respectively).

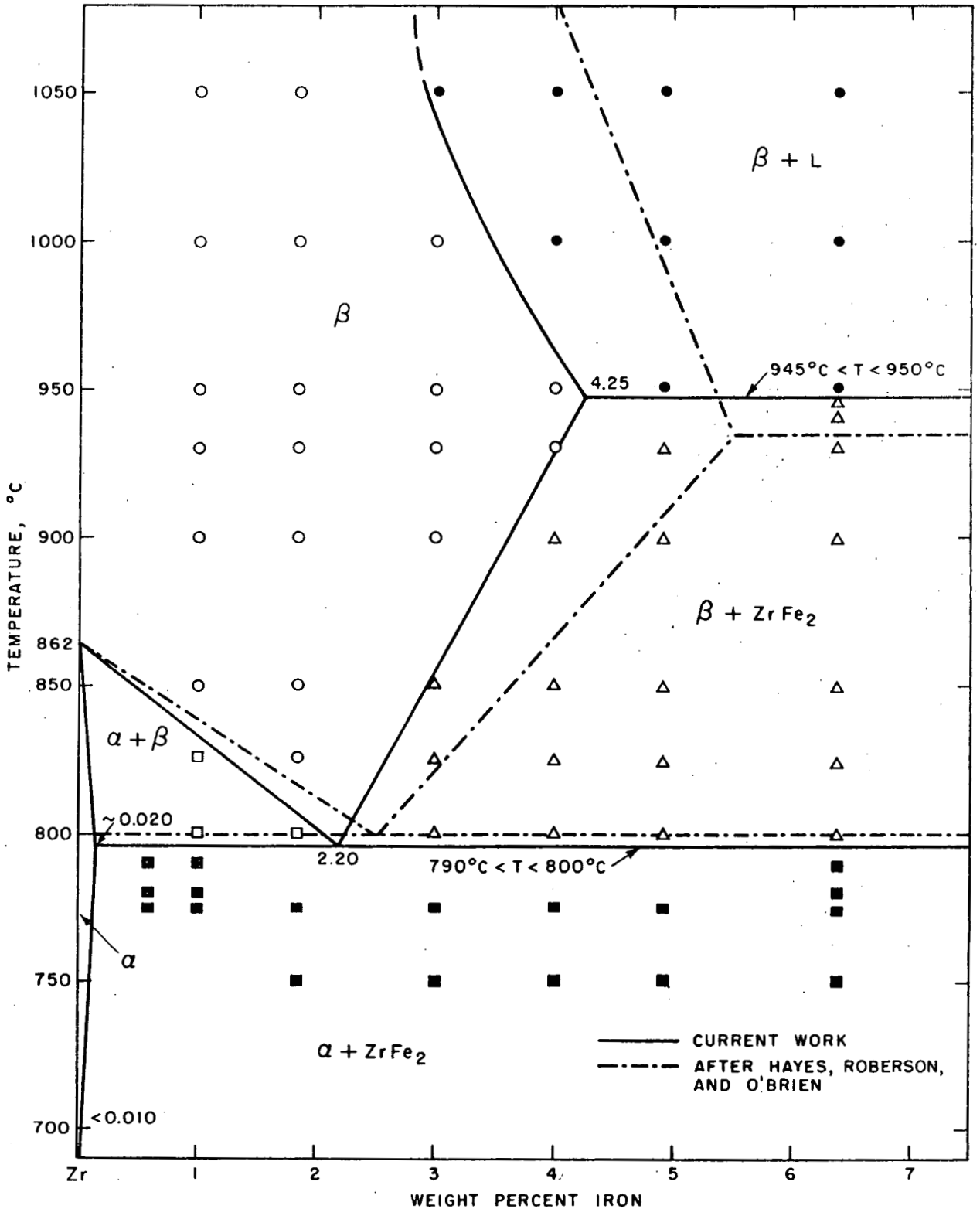

FIG. 7 - THE ZIRCONIUM-RICH CORNER OF THE ZIRCONIUM-IRON SYSTEM

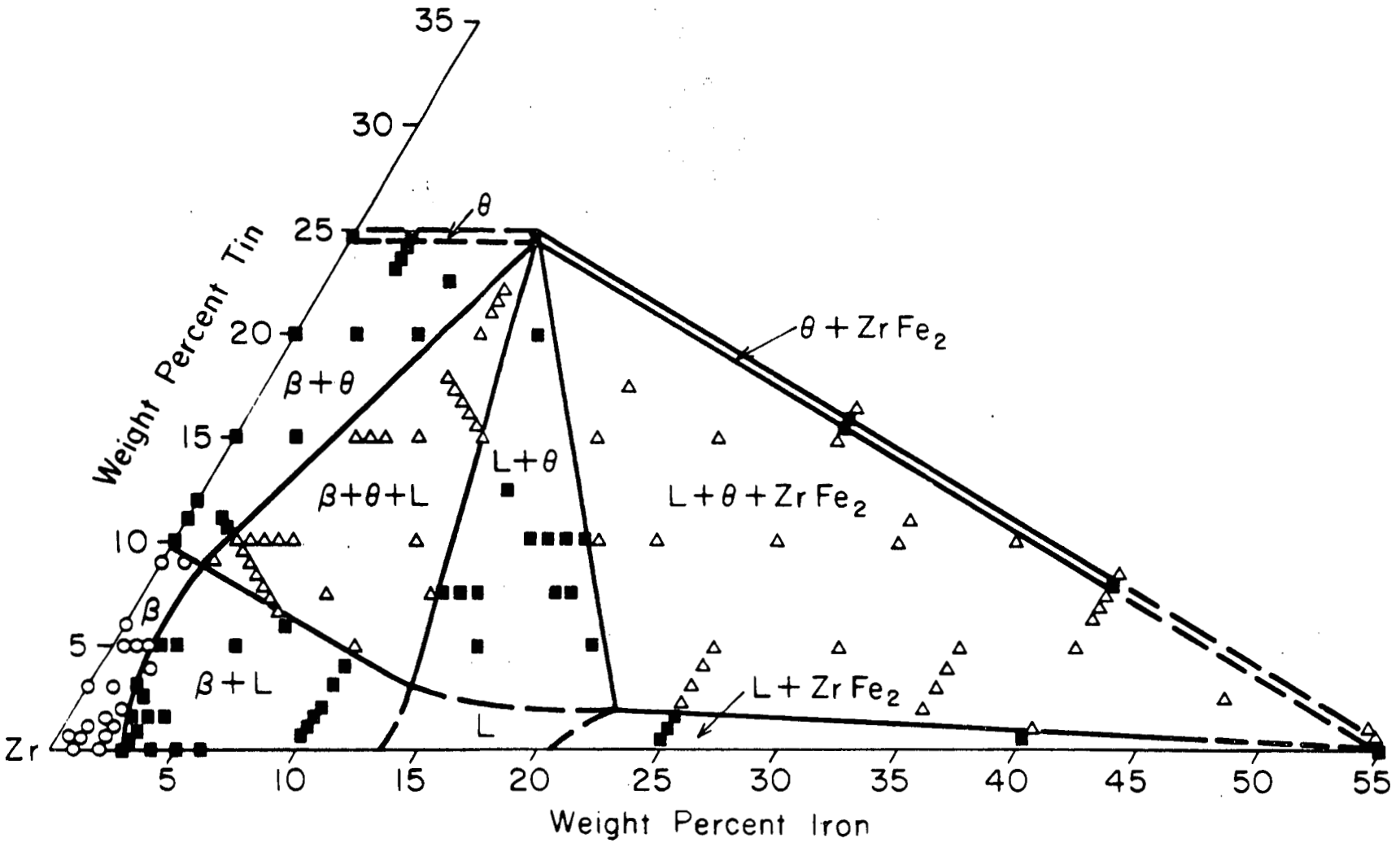

FIG. 8 - PARTIAL ISOTHERMAL SECTION AT 1100°C, Zr-Fe-Sn SYSTEM. OPEN CIRCLE - ONE PHASE; CLOSED SQUARE - TWO PHASES; OPEN TRIANGLE - THREE PHASES.

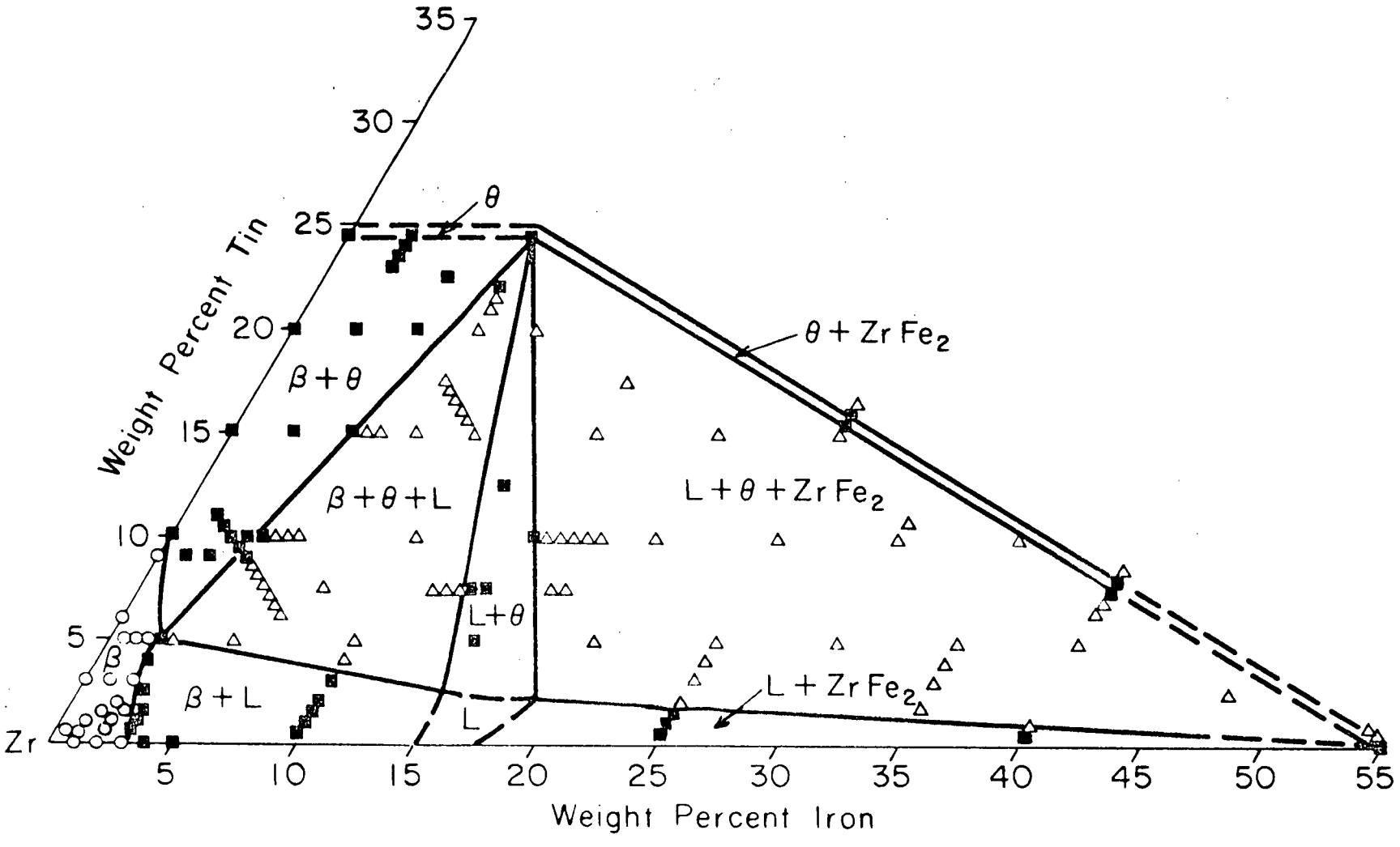

FIG. 9 - PARTIAL ISOTHERMAL SECTION AT 1000°C, Zr-Fe-Sn SYSTEM. OPEN CIRCLE - ONE PHASE; CLOSED SQUARE - TWO PHASES; OPEN TRIANGLE - THREE PHASES.

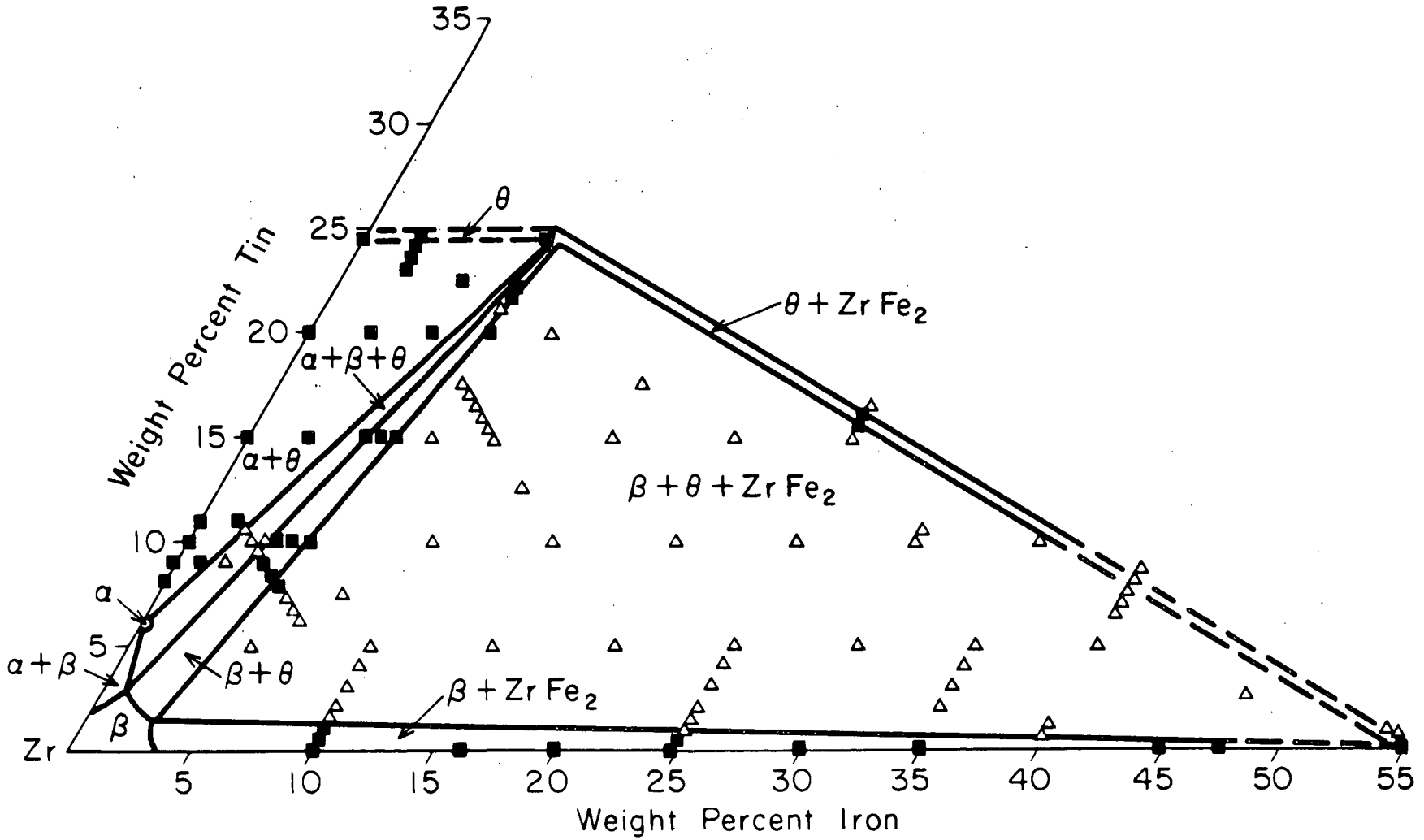

FIG. 10 - PARTIAL ISOTHERMAL SECTION AT 900°C, Zr-Fe-Sn SYSTEM. OPEN CIRCLE - ONE PHASE; CLOSED SQUARE - TWO PHASES; OPEN TRIANGLE - THREE PHASES.

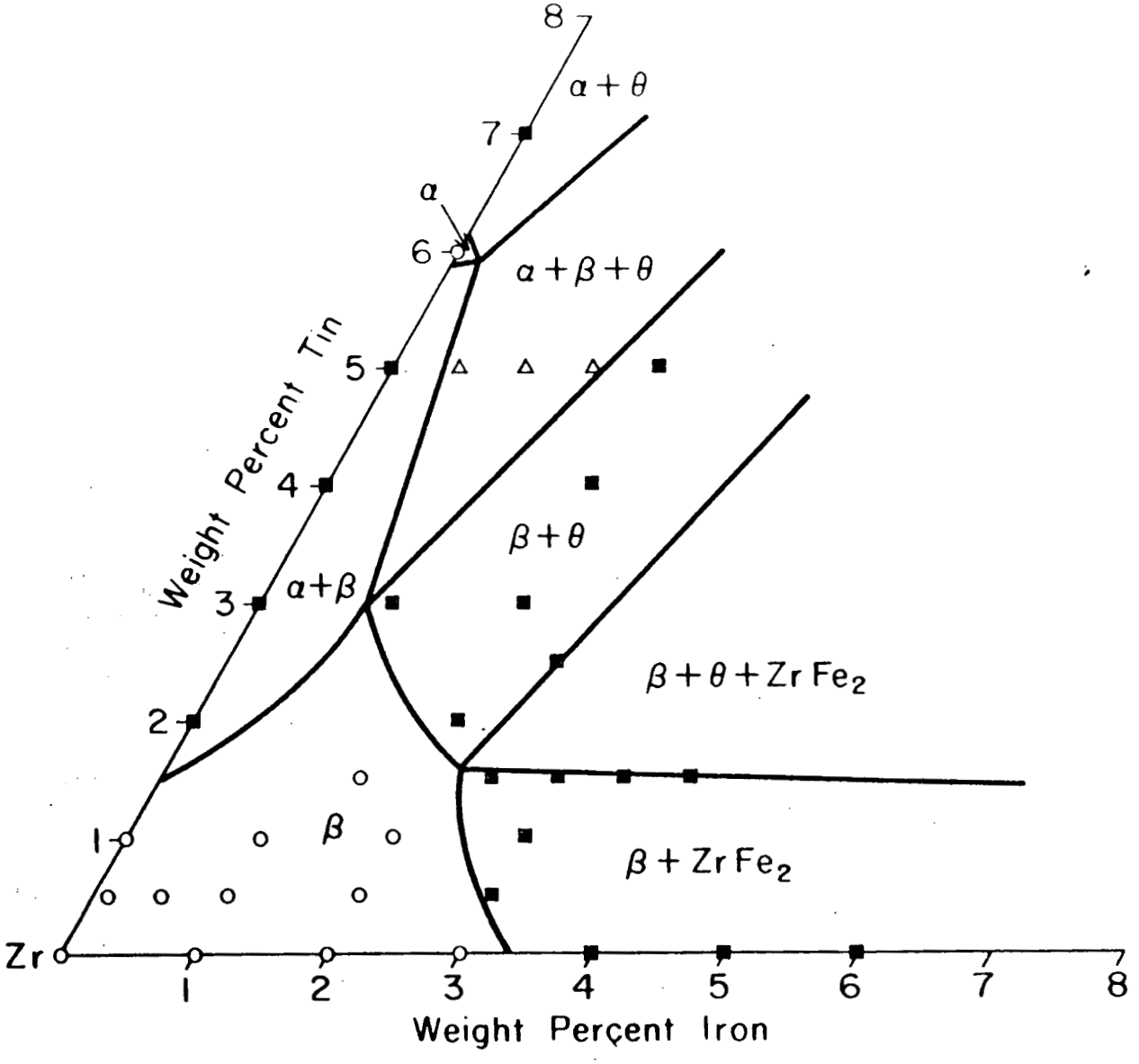

FIG. 11 - PARTIAL ISOTHERMAL SECTION AT 900°C, Zr-Fe-Sn SYSTEM (EXPANDED). OPEN CIRCLE - ONE PHASE; CLOSED SQUARE - TWO PHASES; OPEN TRIANGLE - THREE PHASES.

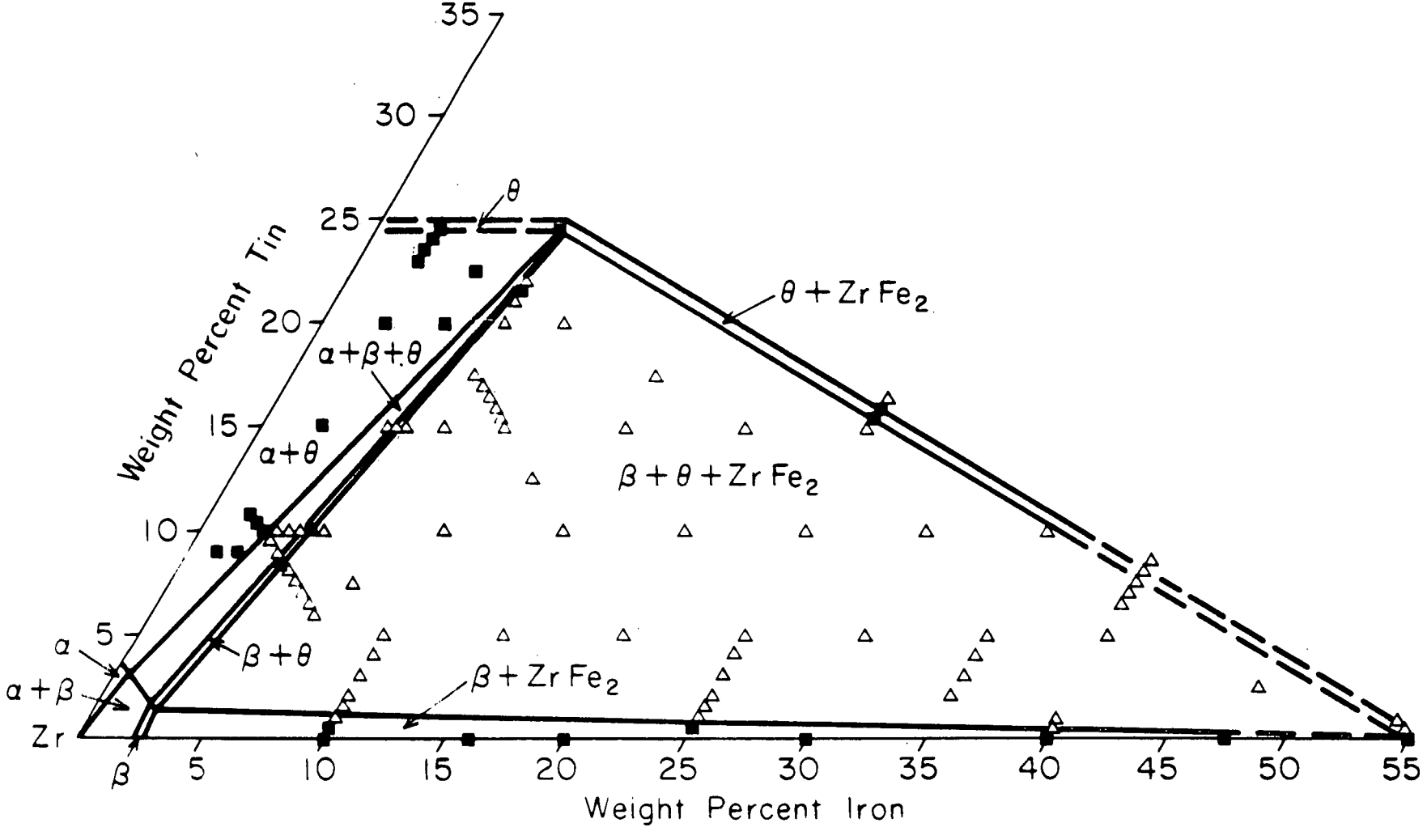

FIG. 12 - PARTIAL ISOTHERMAL SECTION AT 800°C, Zr-Fe-Sn SYSTEM. OPEN CIRCLE - ONE PHASE; CLOSED SQUARE - TWO PHASES; OPEN TRIANGLE - THREE PHASES.

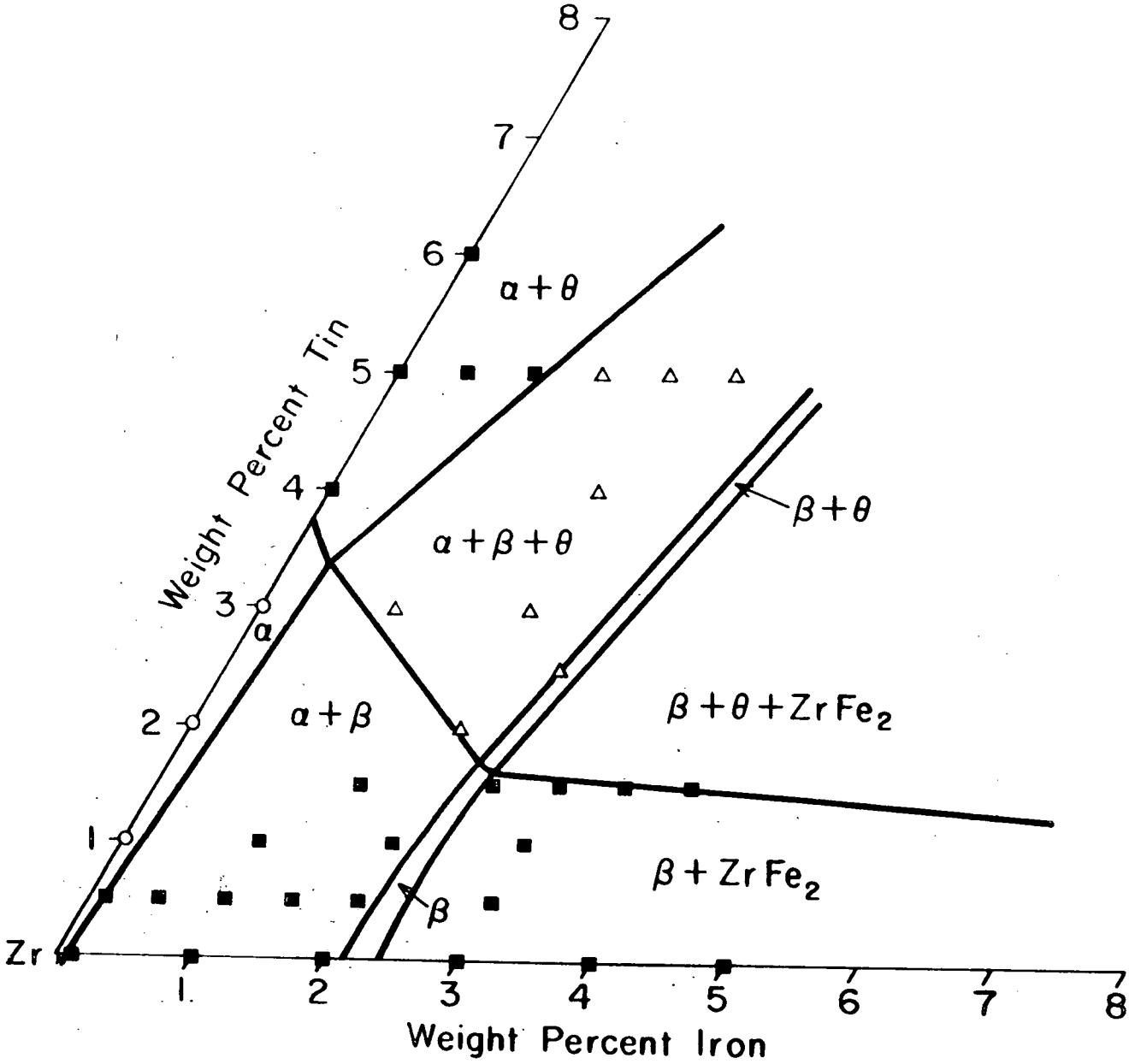

FIG. 13 - PARTIAL ISOTHERMAL SECTION AT 800 °C, Zr-Fe-Sn SYSTEM (EXPANDED). OPEN CIRCLE - ONE PHASE; CLOSED SQUARE - TWO PHASES; OPEN TRIANGLE - THREE PHASES.

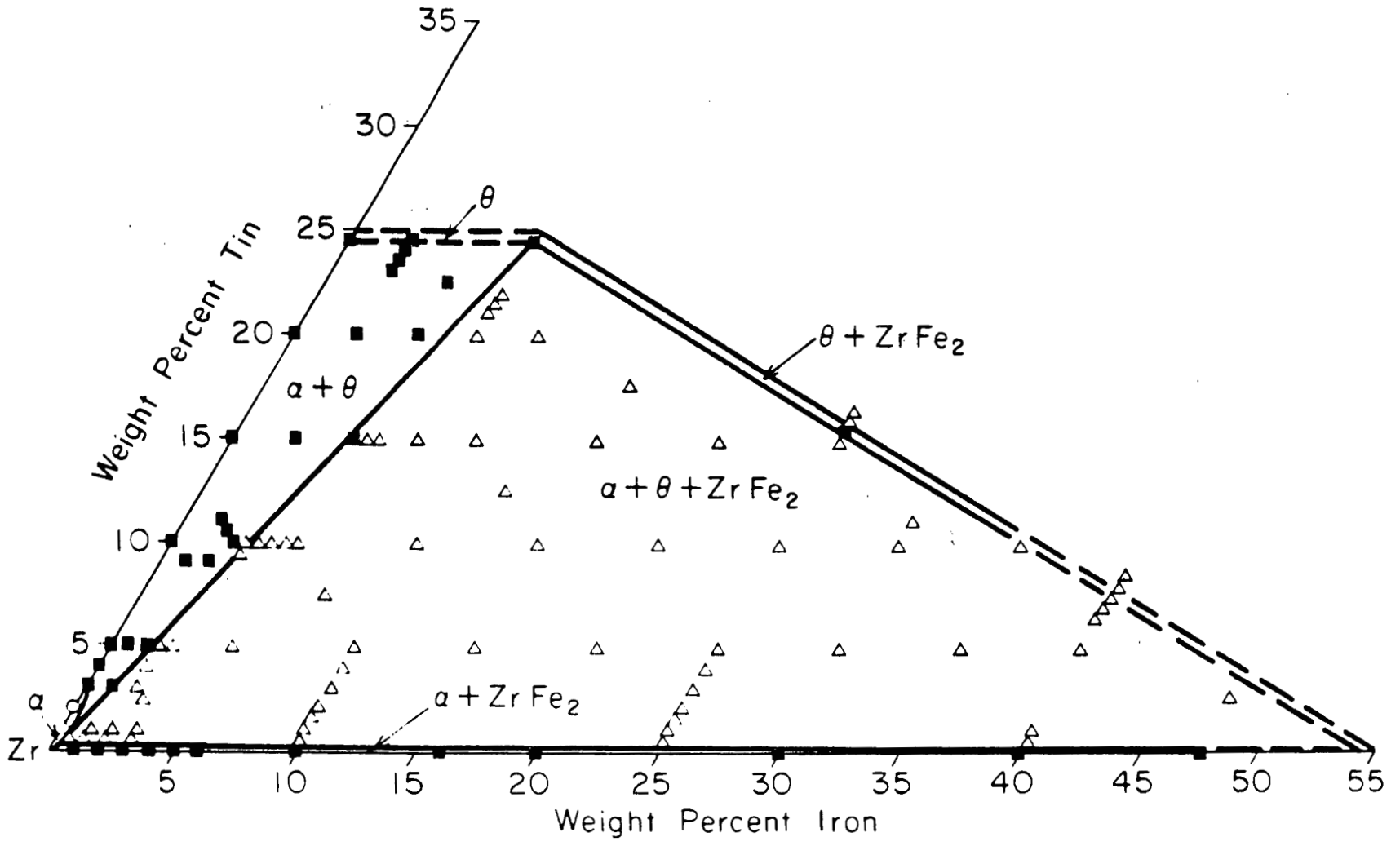

FIG. 14 - PARTIAL ISOTHERMAL SECTION AT 700 °C, Zr-Fe-Sn SYSTEM. OPEN CIRCLE - ONE PHASE; CLOSED SQUARE - TWO PHASES; OPEN TRIANGLE - THREE PHASES.

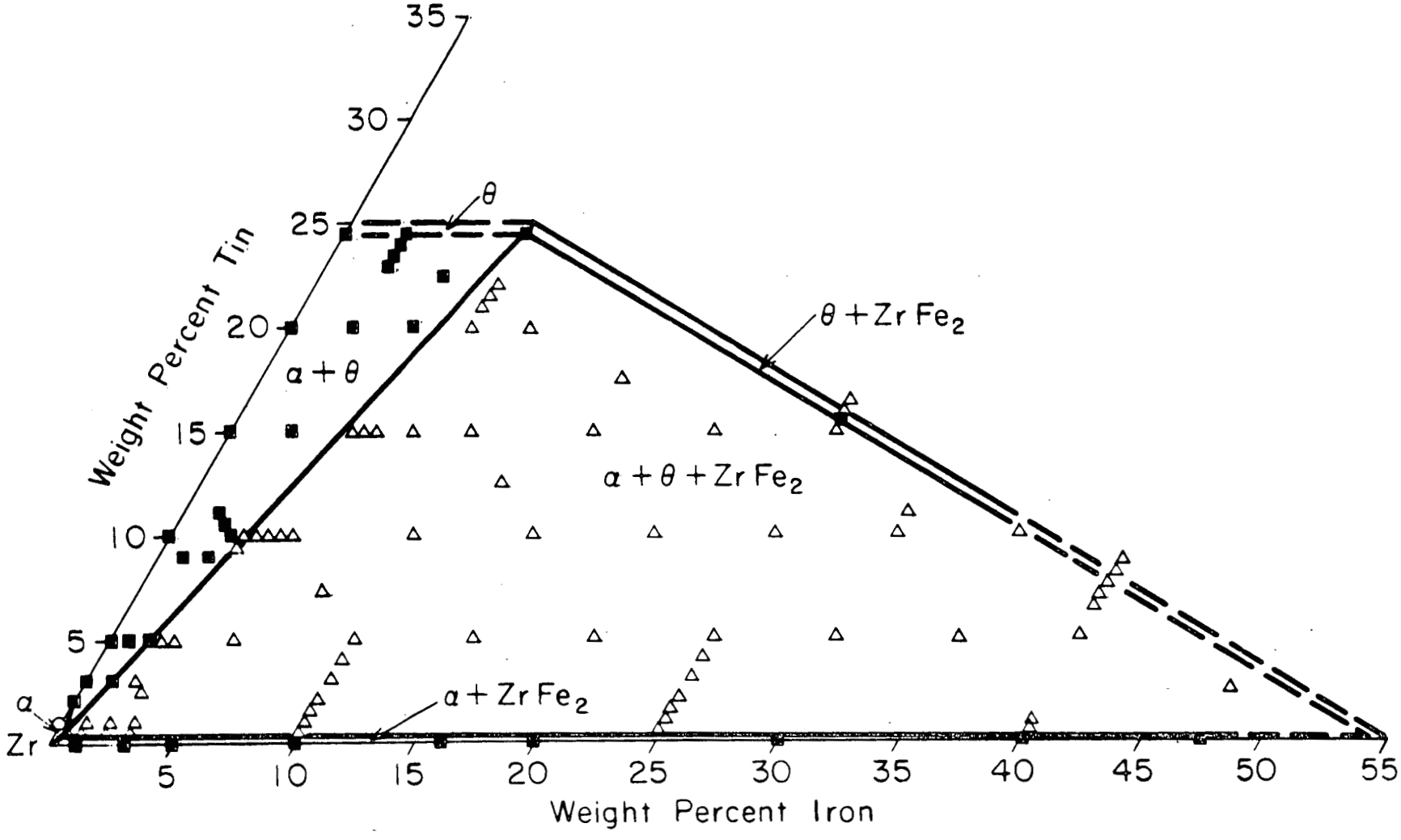

FIG. 15 - PARTIAL ISOTHERMAL SECTION AT 600 °C, Zr-Fe-Sn SYSTEM. OPEN CIRCLE - ONE PHASE; CLOSED SQUARE - TWO PHASES; OPEN TRIANGLE - THREE PHASES.

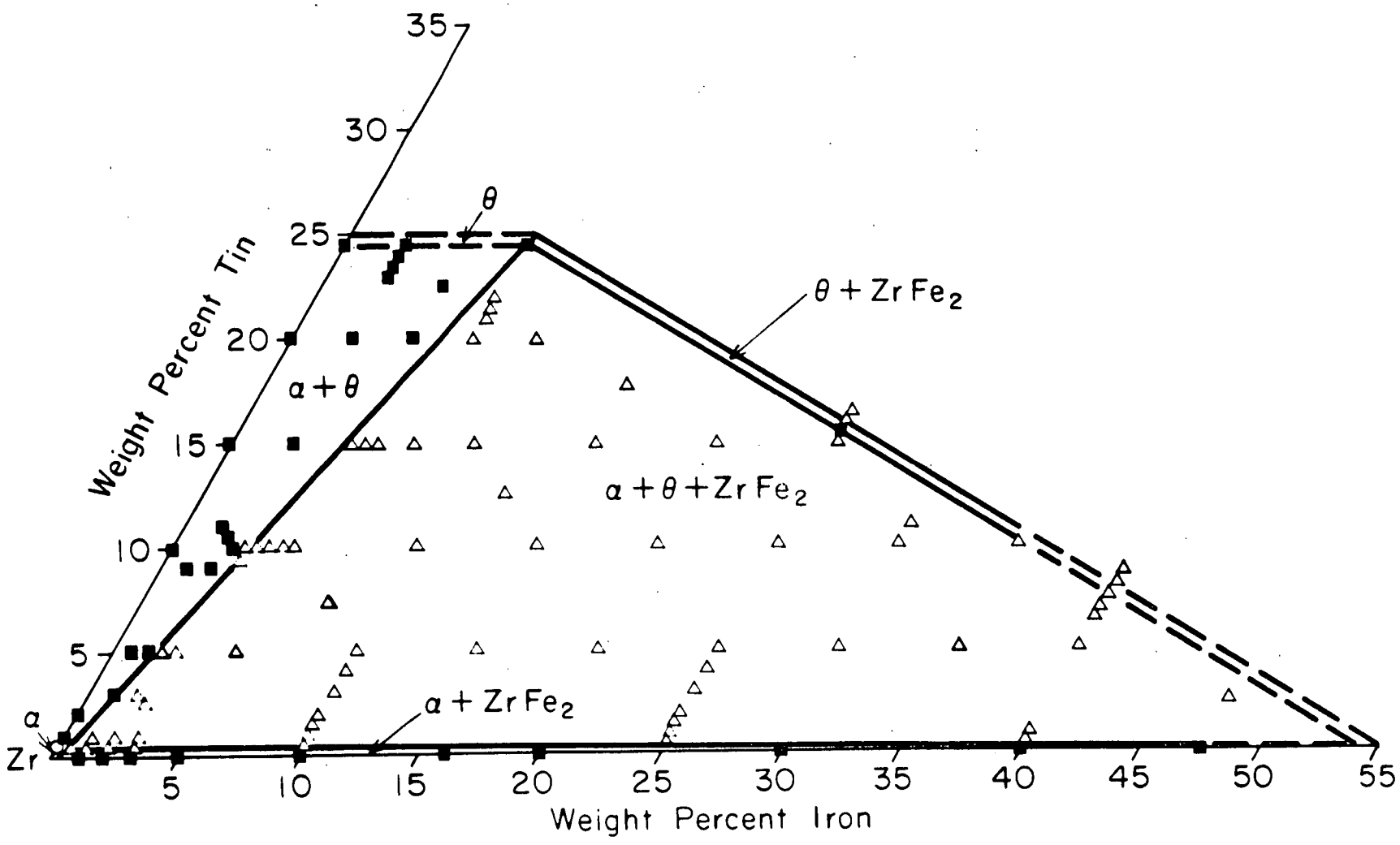

FIG. 16 - PARTIAL ISOTHERMAL SECTION AT 500 °C, Zr-Fe-Sn SYSTEM. OPEN CIRCLE - ONE PHASE; CLOSED SQUARE - TWO PHASES; OPEN TRIANGLE - THREE PHASES.

Metallographic evidence strongly indicates that the theta phase field is a narrow finger extending parallel to the zirconium-iron binary system (at a constant tin composition of about 24.5w/o) indicating the probable substitution of iron for zirconium atoms. The boundaries of this field have not, as yet, been clearly defined; but it appears to be limited to a maximum iron solubility of the order of 7.5w/o. This has been confirmed by Goodwin et al.,[6] who found the iron composition of theta in Zircaloy structures to be in the range of 8 to 10w/o by microanalysis. There seems to be no change in iron solubility with temperature. A nearly single-phase theta structure is seen in Figure 17 of a 7.5w/o Fe, 24.5w/o Sn alloy quenched from 1100°C.

The results of X-ray analysis of this phase were not as definitive. To begin with, after careful study of the d values for Zr_4Sn (from a 24.5w/o Sn alloy), it is felt there is less than satisfactory agreement with the proposed tetragonal lattice.[8] There are indications of its being a structure of lower symmetry, but due to insufficient information, one is not proposed at the present time. Secondly, in the comparison of the diffraction patterns of binary and ternary alloys containing Zr_4Sn (theta), an anomaly in structure becomes evident. In order to discuss this the d values from 7 alloys are presented in Table VII. The d values which could be positively identified as belonging to phases other than the compound in question* have been sorted out. Where identification was questionable due to overlapping, etc., the values were included. It is seen that certain d values would clearly be unique to alpha if the binary sequence were considered alone (i.e., become weaker as the amount of alpha decreases), yet they appear to be quite prominent in the

---

* In general, structures of alloys annealed at 960°C and below contained alpha. The beta in the 5w/o Fe, 15w/o Sn alloy annealed at 1000°C transformed to alpha-prime upon quenching. The 30w/o Fe, 10w/o Sn alloy contained $ZrFe_2$ and liquid at 1000°C besides theta.

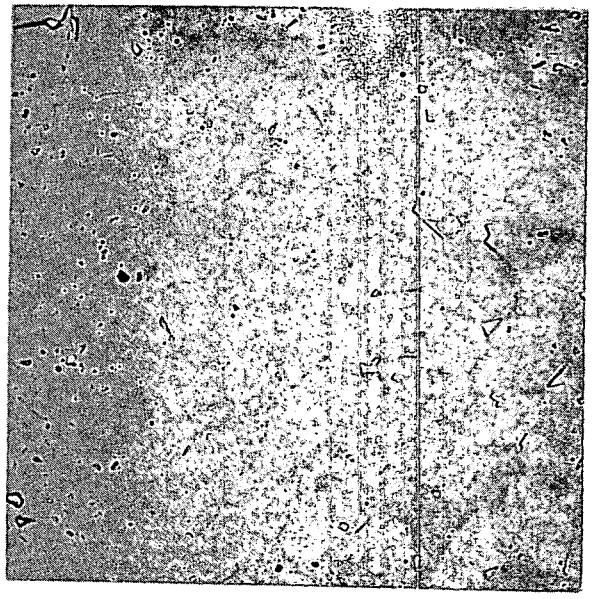

Neg. No. 16204 X 500

Fig. 17

A 7.5w/o Fe, 24.5w/o Sn alloy quenched from 1100°C. Nearly 100% θ plus very small amounts of β.

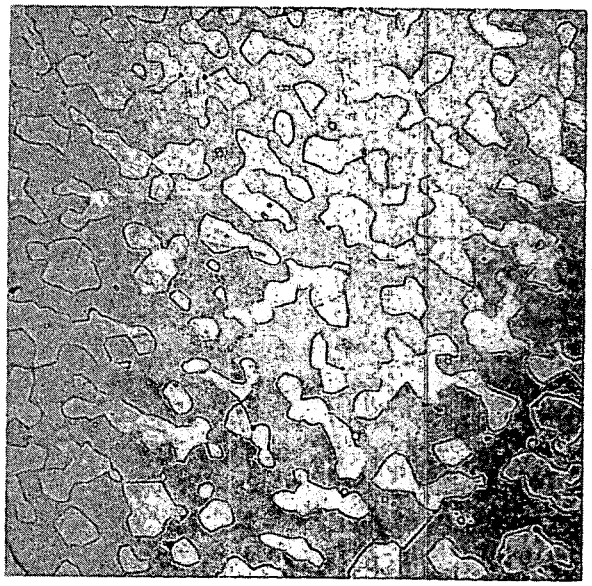

Neg. No. 16200 X 500

Fig. 18

A 25w/o Fe, 15.5w/o Sn alloy quenched from 1100°C. θ plus twinned $ZrFe_2$.

Etchant: 20% HF, 20% HNO_3 in glycerine.

TABLE VII

COMPARISON OF X-RAY DIFFRACTION DATA
FOR THE PHASE Zr_4Sn (θ) FROM ZIRCONIUM-TIN
AND ZIRCONIUM-IRON-TIN ALLOYS

Composition, w/o	Zr-15Sn		Zr-20Sn		Zr-24.5Sn		Zr-5Fe-15Sn		Zr-5Fe-20Sn		Zr-7.5Fe-24.5Sn		Zr-30Fe-10Sn		
Annealing Temperature, °C	960		900		900		1000		900		900		1000		
Quenched Structure	Zr_4Sn+α		Zr_4Sn+α		Zr_4Sn+α		θ+α'		θ+α		θ+α		$ZrFe_2$+θ+L*		
	I	d	I	d	I	d	I	d	I	d	I	d	I	d	Comments
	4	2.771	6	2.782	8	2.790	2	2.767	1	2.775			1	2.74	a
	3	2.591					8	2.592	8	2.608	8	2.595	8	2.60	b,c
	6	2.548	1	2.543									2	2.53	
			8	2.508	9	2.500					6	2.498	7	2.49	d
	9	2.431	5	2.433	4	2.420	9	2.432	9	2.437	7	2.438	7	2.44	
	4	2.282	9	2.281	10	2.291	4	2.294	5	2.289	7	2.288	7	2.29	
	2	2.082					5	2.071	4	2.072	6	2.059	7	2.08	b
	4	1.881	2	1.880	1	1.880	2	1.886			4	1.904	2	1.91	
			4	1.557	8	1.560					2	1.579	3	1.57	a
	1	1.536							1	1.531	2	1.541	2	1.54	
			7	1.496	10	1.500					4	1.506	3	1.50	a
	5	1.455	3	1.455			6	1.450	5	1.440	7	1.439	9	1.44	b,c,d
			3	1.400	7	1.400							2	1.41	a
					1	1.390	5	1.381	3	1.383	6	1.381	8	1.38	b,c

* Solidified liquid.

a Strong in binary alloys; weak or missing in ternary alloys.
b Weak or missing in binary alloys; strong in ternary alloys.
c Could belong to α.
d Belongs to $ZrFe_2$ in Zr-30Fe-10Sn alloy also.

ternary alloys. This is made especially evident in the comparison of the values of the two nearly single-phase alloys (e.g., 24w/o Sn and 7.5w/o Fe, 24.5w/o Sn). These lines are missing in the binary compound but are very intense in the ternary compound. This was also true when comparing 24.5w/o Sn alloys containing smaller amounts of iron (2.5 and 5w/o) with the binary compound.

In general, there is a change in the relative intensities of all lines when going from the binary to the ternary compound, but this could be expected in a continuous phase which is replacing one of its atoms with a new species. However, it is difficult to justify the absence of certain lines in the binary compound which are intense in the ternary and vice versa. If all the values presented were considered to be unique to Zr_4Sn (theta), it would appear as if the binary alloys, with the exception of the one containing 24.5w/o Sn, are similar to the ternaries. Assuming theta to be a continuous phase, which is borne out by metallographic evidence, this could be indicative of allotropy. Further investigation would be necessary to resolve this problem.

The θ + $ZrFe_2$ field was found to be quite narrow. A typical structure is shown in Figure 18 of a 25w/o Fe, 15.5w/o Sn alloy quenched from 1100°C. Extrapolation of this field from the end of the theta field indicates that the $ZrFe_2$ field should exist in the vicinity of 55w/o Fe in the zirconium-iron binary. This is contrary to the reported 47.5w/o Fe,[5] though stoichiometrically it would be expected at 55w/o. There was no metallographic evidence to establish it at either composition, while X-ray evidence tends to confirm the latter composition. This was seen by comparing diffraction patterns made of 47.5w/o Fe alloy with those of the stoichiometric composition made by Elliott.[8] The patterns were identical except for stray lines found only in the patterns of the 47.5w/o Fe alloy.

The solubility for tin in $ZrFe_2$ is quite small, as is evidenced by the difficulty in locating the single-phase field in ternary alloys. This is also confirmed by the fact that the $\alpha + ZrFe_2/\alpha + ZrFe_2 + \theta$ phase boundary lies inside the most tin-dilute ternary alloys prepared.

The liquid to solid transformation was studied more closely, and it appears to be a four-phase ternary eutectic, $L \rightleftharpoons \beta + \theta + ZrFe_2$, at a temperature between 930° and 935°C. Evidence of this transformation is seen in the structures of a 13w/o Fe, 7.5w/o Sn alloy quenched from 935° and 930°C (Figures 19 and 20, respectively).

A four-phase ternary peritectoid, $\beta + \theta \rightleftharpoons \alpha + ZrFe_2$, at a temperature below 800°C but above the zirconium-iron binary eutectoid (which lies between 790° and 800°C), seems to be the most logical solid-state transformation. However, metallographic evidence in this case is more difficult to obtain due to the refinement of phases at these temperatures, etc. Therefore, a four-phase ternary eutectoid, $\beta \rightleftharpoons \alpha + \theta + ZrFe_2$, at a temperature just below the zirconium-iron binary eutectoid remains an alternate possibility.

2. Alpha Solubility

a. Magnetic Susceptibility

The susceptibility of paramagnetic and diamagnetic samples is independent of the magnetic field strength. However, when small amounts of ferromagnetic components are imbedded in a nonferromagnetic matrix, the apparent susceptibility of the combination may be shown to obey a relationship of the form:[4]

$$k_H = k_\infty + CM_S/H,$$

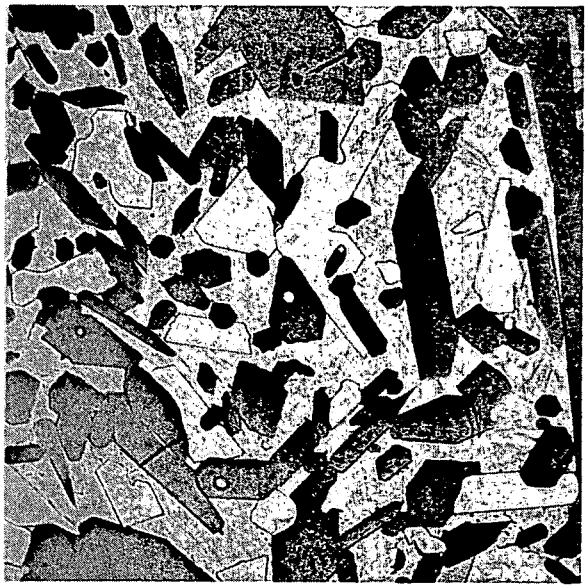

Neg. No. 16195 X 250

Fig. 19

A 13w/o Fe, 7.5w/o Sn alloy quenched from 935°C. θ (dark phase) and $ZrFe_2$ (white, twinned phase) rejected from liquid.

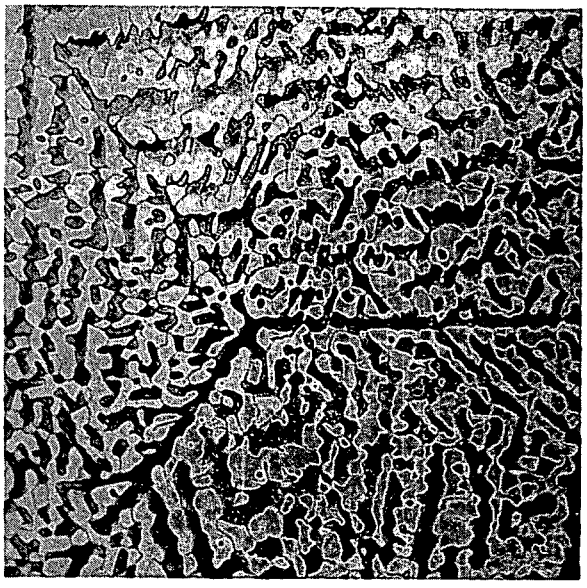

Neg. No. 16198 X 500

Fig. 20

A 13w/o Fe, 7.5w/o Sn alloy quenched from 930°C. Eutectic of β + θ + $ZrFe_2$.

Etchant: 20% HF, 20% HNO_3 in glycerine.

where k_H is the apparent susceptibility at field strength H,
k_∞ is the true susceptibility of the matrix,
C is the concentration of the ferromagnetic component,
and M_S is its saturation magnetic moment.

According to this equation, a plot of measured susceptibility versus 1/H should yield a straight line. The magnitude of the slope (CM_S) is a measure of the amount of ferromagnetic material present. Furthermore, the intercept, k_∞, is the true susceptibility of the matrix.

The results of these tests are summarized in Table VIII and in Figure 21. The susceptibility of pure zirconium is reported to be of the order of 1.3 to 1.4 x 10^{-6} emu/gram[9] which agrees favorably with the value determined in this study (1.5 x 10^{-6} emu/gram). It is seen that within the sensitivity of this apparatus the technique is effective in determining the presence of $ZrFe_2$ when this compound appears in substantial amounts. The microstructure of the two 3-phase alloys (1w/o Fe, 0.5w/o Sn and 1w/o Fe, 1w/o Sn) showed smaller amounts of $ZrFe_2$ than found in the 1w/o Fe alloy. Thus, this technique is not considered sensitive enough for further work with the extremely dilute alloys of this investigation since even smaller quantities of $ZrFe_2$ would be expected in these alloys.

b. Metallography

Homogenization at 800°C produced large-grained alpha structures in a majority of the dilute alloys. The remaining alloys exhibited small amounts of beta at grain boundaries and grain corners. A partial isothermal section at 800°C is presented in Figure 22.

Examination of specimens quenched after 429 hours at 400°, 450° and 500°C revealed that in those alloys having beta at 800°C the beta was not, as yet, decomposed. Samples given longer anneals (i.e., >1000 hours) at temperatures

TABLE VIII

SUSCEPTIBILITY MEASUREMENTS OF ZIRCONIUM-BASE ALLOYS

Composition				
w/o Fe	w/o Sn	Heat Treatment	Structure	Results
0	0	600 hr-600°C-WQ	α	paramagnetic*
0	24.5	150 hr-700°C-WQ	nearly 100% Zr_4Sn (θ) + α	paramagnetic
1	0	300 hr-750°C-WQ	α + $ZrFe_2$	ferromagnetic
5	0	600 hr-600°C-WQ	α + $ZrFe_2$	ferromagnetic
1	0.5	744 hr-600°C-WQ	α + θ + $ZrFe_2$	paramagnetic
1	1	744 hr-600°C-WQ	α + θ + $ZrFe_2$	paramagnetic
1	9	744 hr-600°C-WQ	α + θ	paramagnetic
2.5	15	508 hr-700°C-WQ	α + θ	paramagnetic

* All paramagnetic samples have a susceptibility of the order of 1.5×10^{-6} emu/gram.

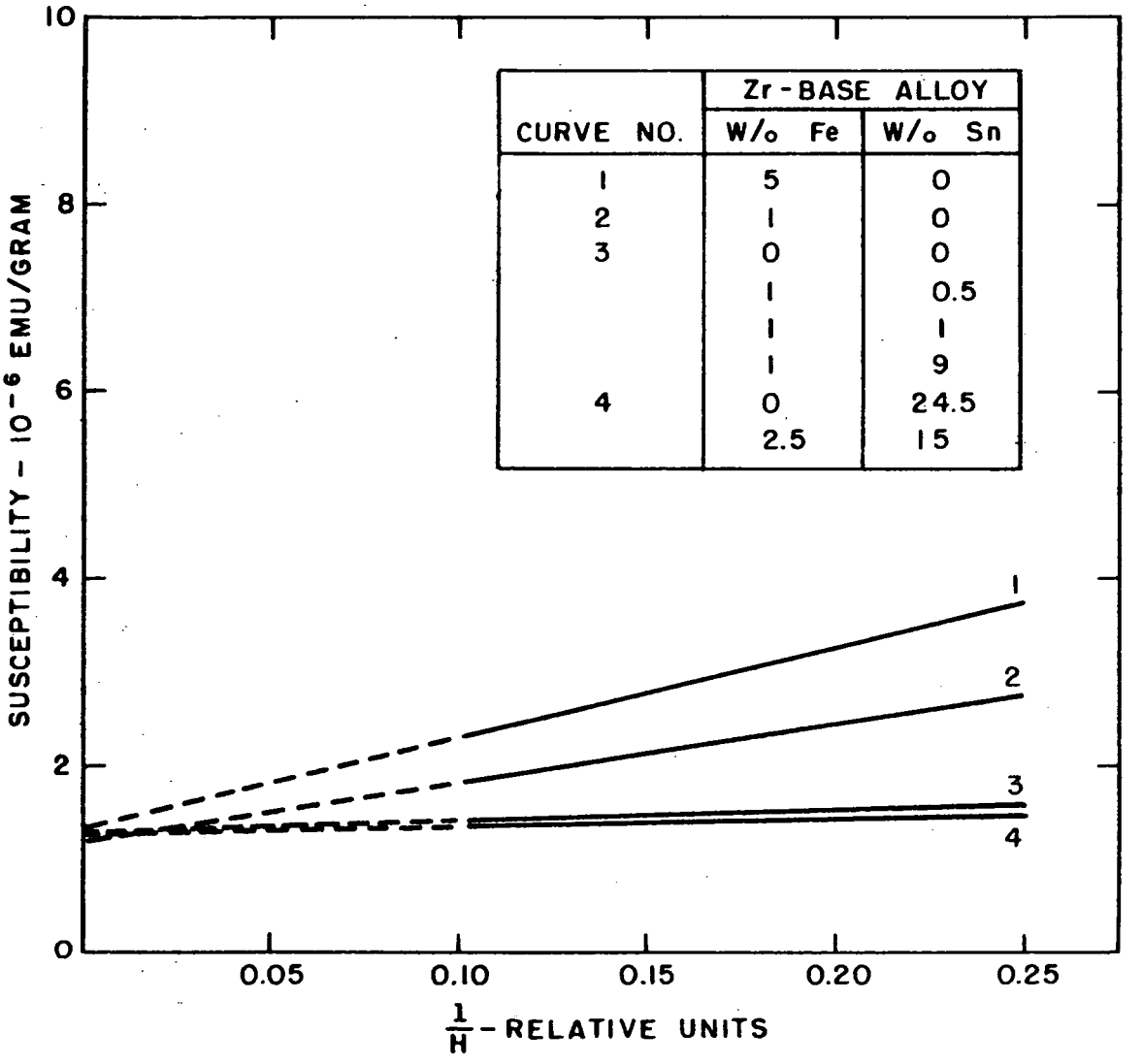

FIG. 21 - SUSCEPTIBILITY OF ZIRCONIUM-BASE ALLOYS AS A FUNCTION OF RECIPROCAL MAGNETIC FIELD

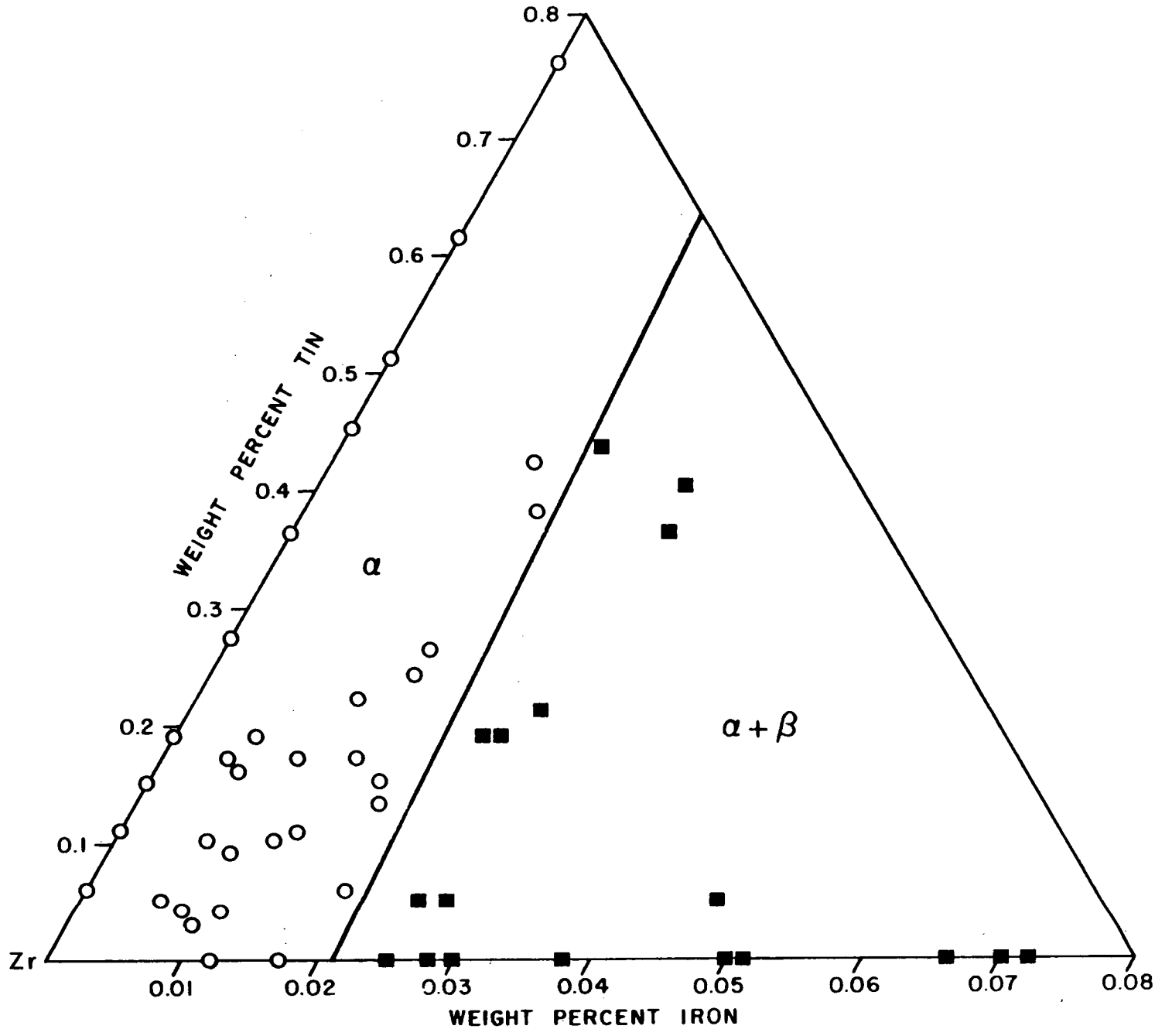

FIG. 22 - ZIRCONIUM-RICH CORNER OF THE Zr-Fe-Sn SYSTEM AT 800°C. OPEN CIRCLE - ONE PHASE; CLOSED SQUARE - TWO PHASES.

as low as 400°C appeared to have reached equilibrium. Evidences of incomplete recrystallization as well as some undecomposed beta were observed in structures of some alloys annealed at lower temperatures for extended periods of time. However, this did not prove to be a critical problem since the alpha phase boundary was found to be below the most dilute binary iron and ternary alloys prepared at 600°C and lower. A partial isothermal section for 700°C appears in Figure 23. The $\alpha + \theta/\alpha + \theta + ZrFe_2$ boundary was extrapolated from the higher composition area of the diagram where it is firmly established. The similarity of the precipitating phases, when they are present in such limited quantity, made it difficult to establish positive identifications except when the phase appeared in binary alloys. Therefore, the half-open circles represent ternary alloys which contain a precipitate as opposed to the open circles which represent single-phase alloys and closed squares representing two-phase binary alloys. The alpha phase boundaries for the temperatures 600°C and below are proposed in Figure 24 where only the binary tin alloys provided solubility data besides the upper limit of ternary solubility set by the most dilute ternary alloys.

The following series of photomicrographs illustrate the type of structures encountered in these alloys. Figure 25 shows $ZrFe_2$ precipitate particles running in transgranular paths in the most dilute iron binary alloy (0.012w/o) quenched from 700°C. This indicates precipitation took place along slip bands prior to recrystallization in the heavily cold-worked material. This behavior was found to be typical of all the alloys. Also present in most of the specimens were hydride platelets which appeared within the grains as well as at grain boundaries. It is difficult to be sure whether the more refined particles found in Figure 25 are the same as those found in unalloyed

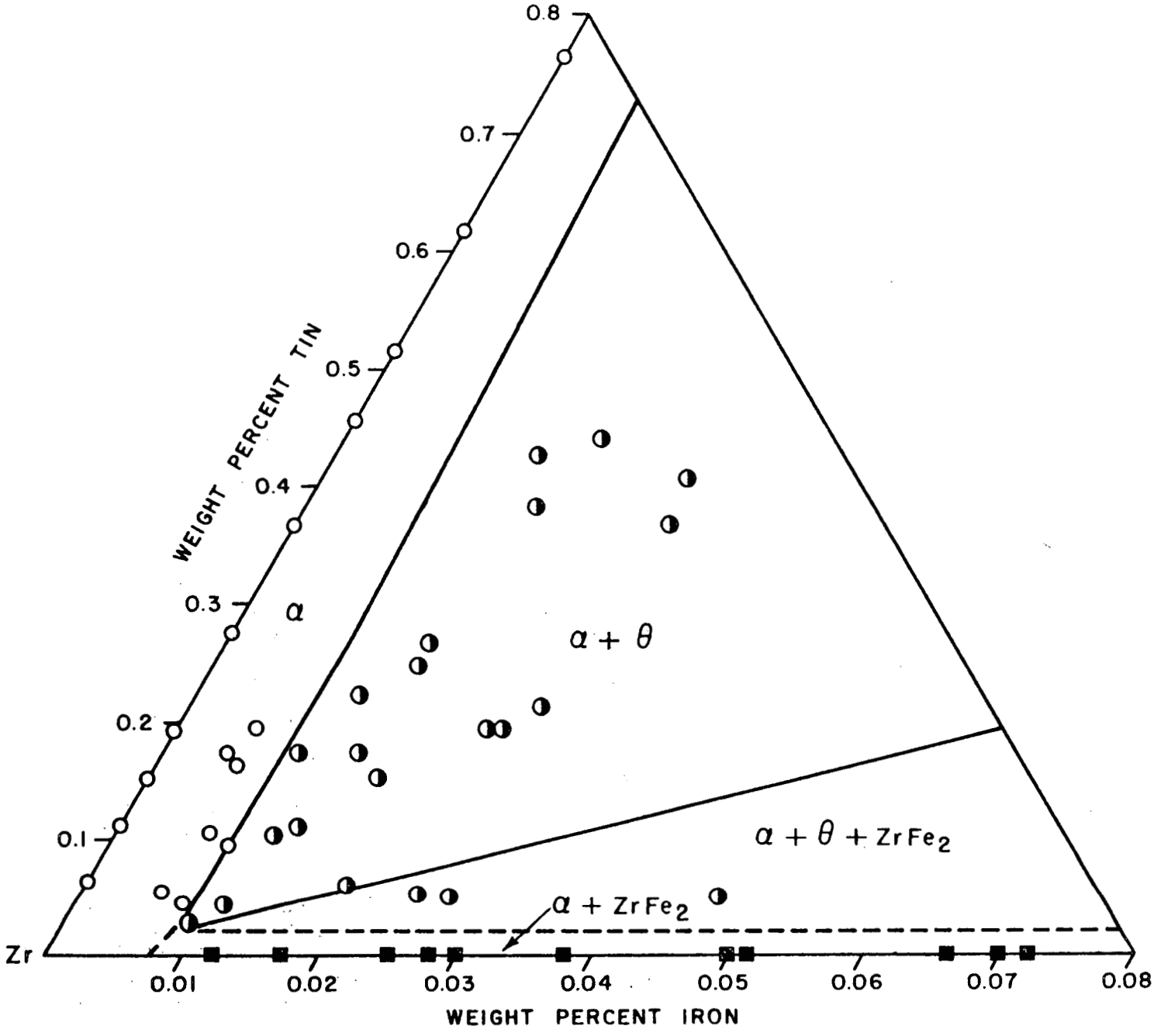

FIG. 23 - ZIRCONIUM-RICH CORNER OF THE Zr-Fe-Sn SYSTEM AT 700°C. OPEN CIRCLE - ONE PHASE; CLOSED SQUARE - TWO PHASES; HALF OPEN CIRCLE - TWO OR THREE PHASES.

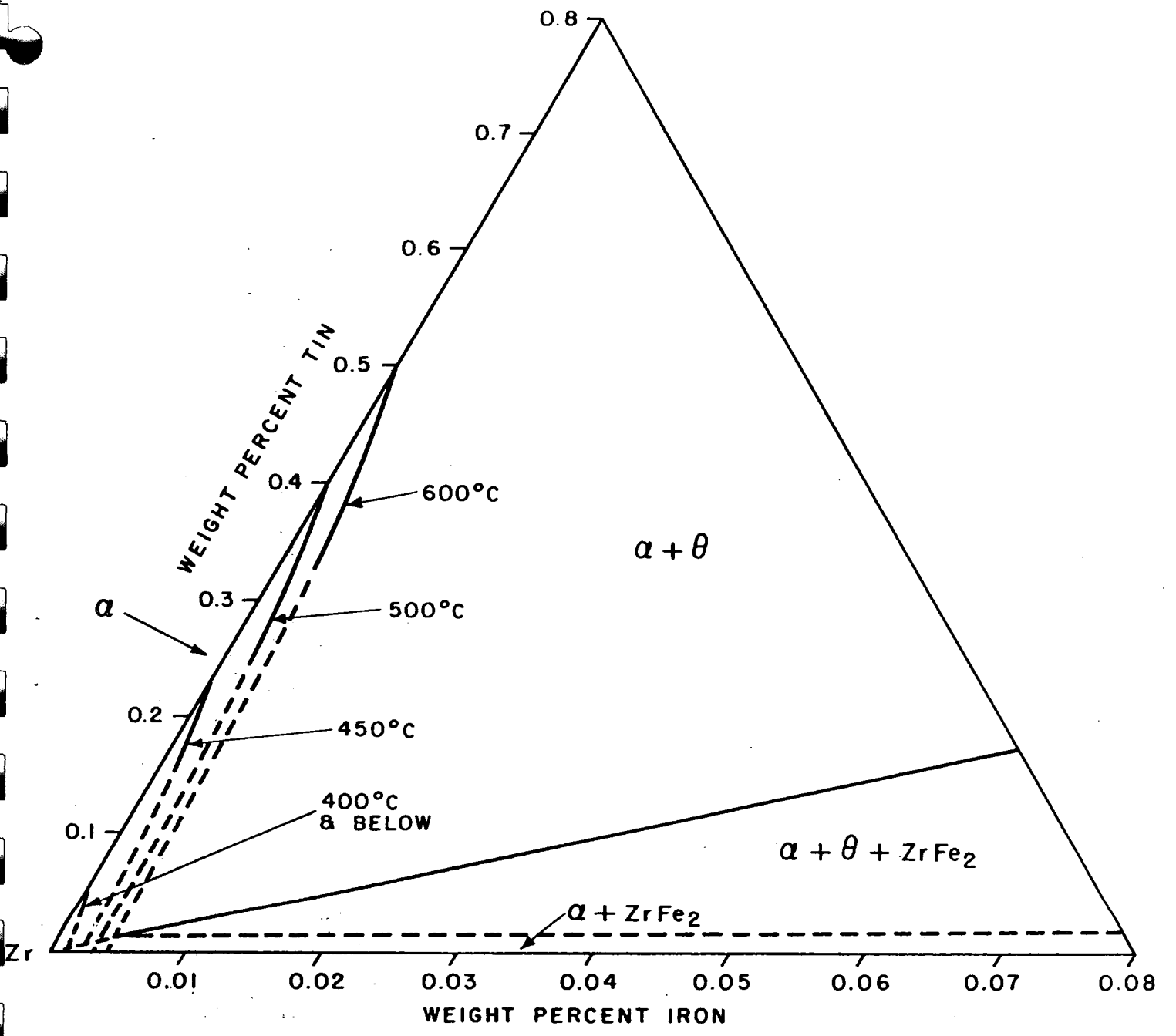

FIG. 24 - ZIRCONIUM-RICH CORNER OF THE Zr-Fe-Sn SYSTEM AT 600°, 500°, 450° AND 400°-200°C

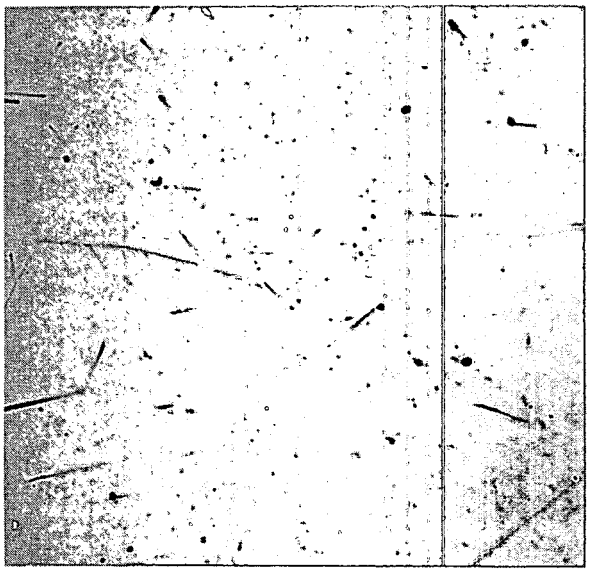

Neg. No. 16470 X 1000

Fig. 25

A 0.012w/o Fe alloy quenched from 700°C. α + $ZrFe_2$ structure; some hydride platelets in evidence.

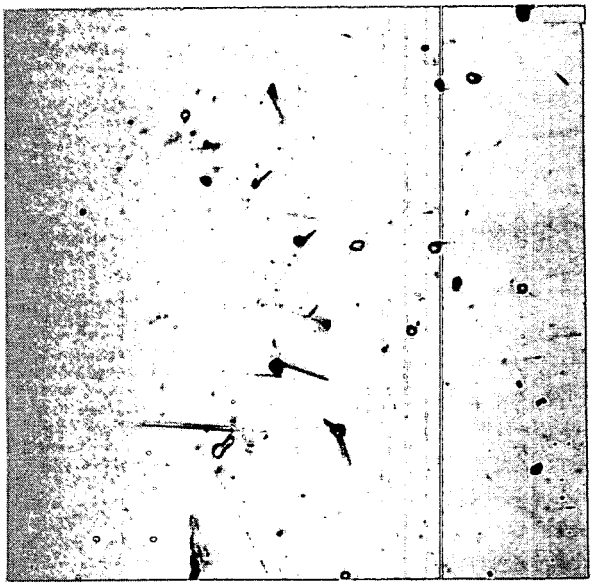

Neg. No. 16468 X 1000

Fig. 26

A 0.052w/o Fe alloy quenched from 700°C. α + $ZrFe_2$ structure; some hydride platelets in evidence.

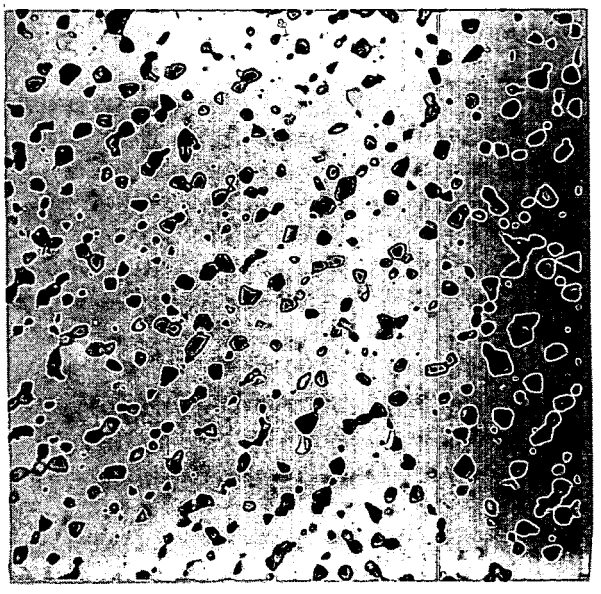

Neg. No. 15235 X 250

Fig. 27

A 2w/o Fe alloy quenched from 775°C. α + $ZrFe_2$ structure.

Etchant: 20% HF, 20% HNO_3 in glycerine; 50% H_2O_2, 45% HNO_3, and 5% HF.

zirconium* and thus determine whether they are hydride or $ZrFe_2$. The particle size of $ZrFe_2$ seems to increase with increasing amounts of iron as is evident in the 0.052w/o Fe alloy quenched from 700°C (Figure 26). Typical $ZrFe_2$ in an alloy of higher iron content is seen in Figure 27 (2w/o Fe, quenched from 775°C).

A relatively clean alpha structure is seen in Figure 28 of 0.76w/o Sn alloy quenched from 700°C. Precipitation of Zr_4Sn is observed in a 0.45w/o Sn alloy quenched from 500°C (Figure 29), and it can be seen that it is quite similar to $ZrFe_2$ in Figures 25 and 26. There seems to be a tendency toward more nucleation and less growth on the part of Zr_4Sn, as seen in a 5w/o Sn alloy quenched from 700°C (Figure 30), when compared to $ZrFe_2$ in Figure 27. The particles in the structure of a 0.028w/o Fe, 0.36w/o Sn alloy quenched from 700°C (Figure 31) are assumed to be $\theta(Zr_4Sn)$ due to its position in the $\alpha + \theta$ phase field determined by the earlier work. However, identification from metallographic observation alone would be impossible.

A few very dilute ternary alloys at 700°C possessed a single-phase alpha structure. Typical of the alloys which bracket the $\alpha/\alpha + \theta$ phase boundary are the one with 0.008w/o Fe, 0.07w/o Sn having a relatively dirty alpha structure (Figure 32) and the one with 0.012w/o Fe, 0.10w/o Sn having an $\alpha + \theta$ structure (Figure 33).

V. SUMMARY

The zirconium-iron-tin system up to the first compound in the binary systems ($ZrFe_2$ and Zr_4Sn) between 500° and 1100°C as presented in last year's summary report was thoroughly checked. The proposed phase relations were confirmed, and phase boundaries were adjusted to their proper positions. The

---

* Discussed in Section IV, part A.

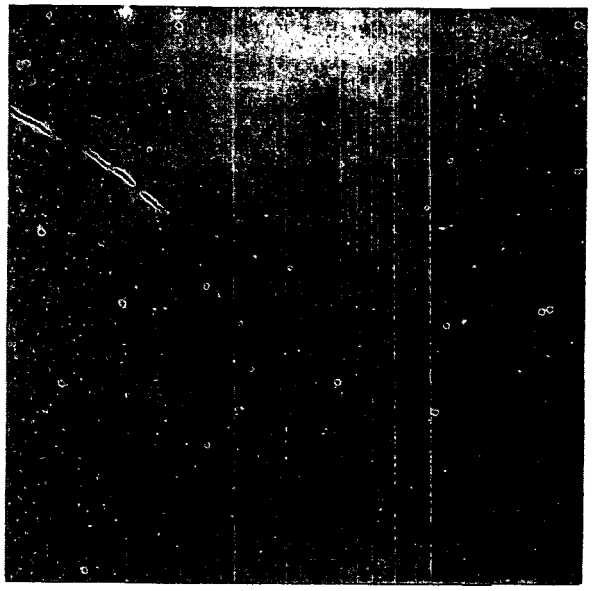

Neg. No. 16475 X 1000

Fig. 28

A 0.76w/o Sn alloy quenched from 700°C. Single-phase α structure.

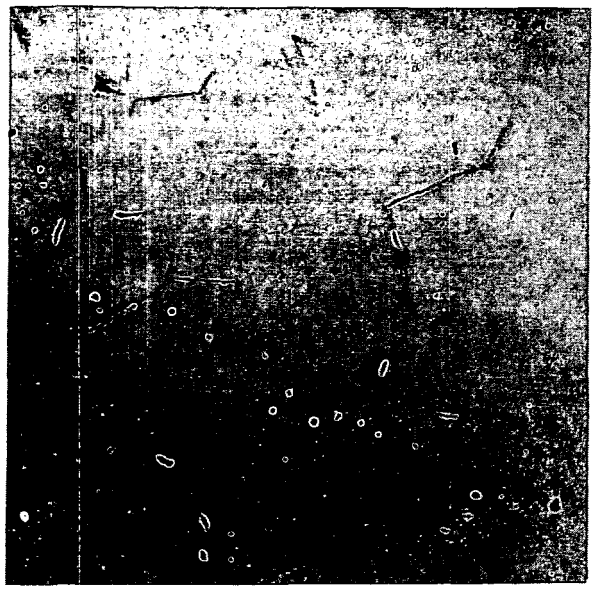

Neg. No. 16474 X 1000

Fig. 29

A 0.45w/o Sn alloy quenched from 500°C. α + Zr_4Sn; some hydride platelets in evidence.

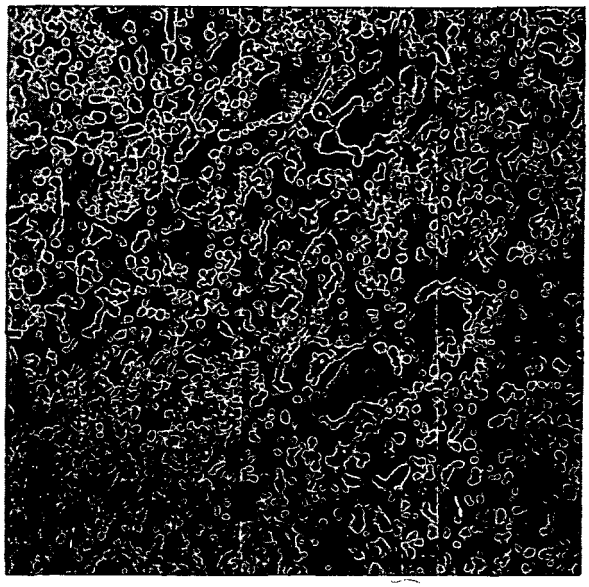

Neg. No. 16467 X 1000

Fig. 30

A 5w/o Sn alloy quenched from 700°C. α + Zr_4Sn structure.

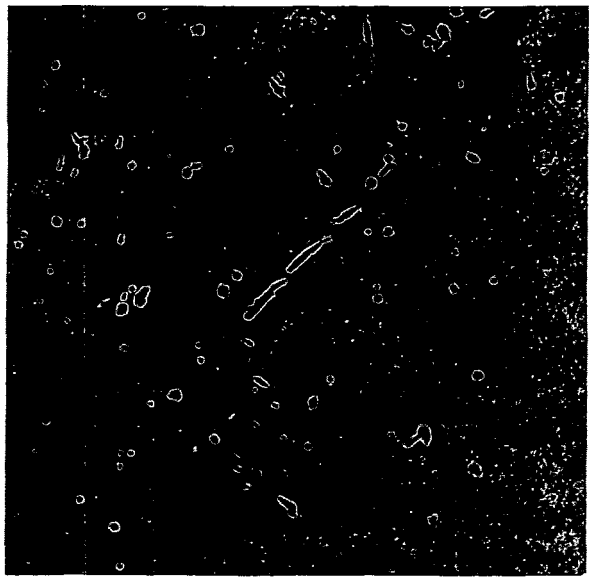

Neg. No. 16469 X 1000

Fig. 31

A 0.028w/o Fe, 0.36w/o Sn alloy quenched from 700°C. α + θ structure; some hydride in evidence.

Etchant: 20% HF, 20% HNO_3 in glycerine; 50% H_2O_2, 45% HNO_3, and 5% HF.

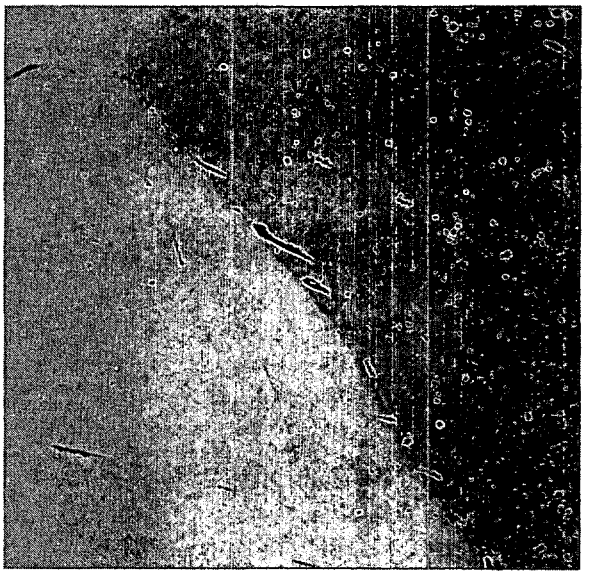

Neg. No. 16475 X 1000

Fig. 32

A 0.008w/o Fe, 0.070w/o Sn alloy quenched from 700°C. Single-phase α structure; some hydride in evidence.

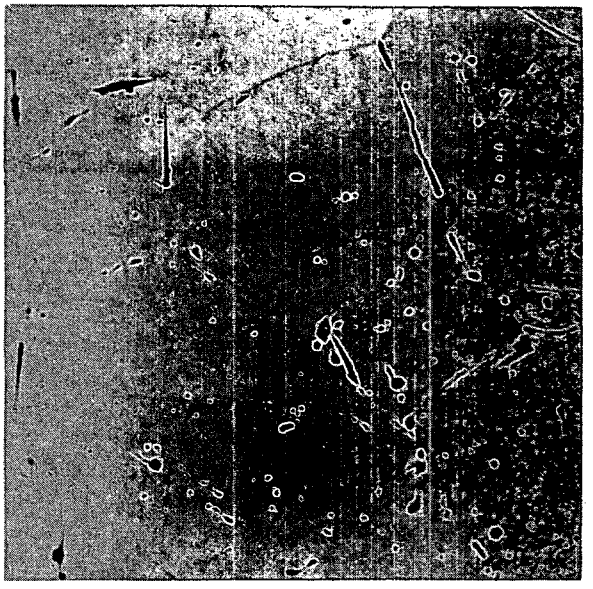

Neg. No. 16471 X 1000

Fig. 33

A 0.012w/o Fe, 0.10w/o Sn alloy quenched from 700°C. α + θ structure; some hydride in evidence.

Etchant: 20% HF, 20% HNO_3 in glycerine; 50% H_2O_2, 45% HNO_3, and 5% HF.

results are described in 9 isothermal sections (Figures 8 through 16). The solubility of iron and tin in alpha-zirconium between 200° and 800°C was also studied, and these results appear in Figures 22 through 24. The zirconium-rich portion of the zirconium-iron system based on iodide material is also presented (Figure 7).

The details of melting and heat treating procedures for the alloys of this system are described. Metallographic, X-ray, and magnetic susceptibility techniques are discussed.

The following are the important features of the system:

(1) There is little solubility for tin in the compound $ZrFe_2$. The single-phase field is believed to exist in the vicinity of 55w/o Fe.

(2) The compound theta appears to be a continuous phase originating at the binary compound (Zr_4Sn) and dissolving up to about 7.5w/o Fe while maintaining a constant tin composition of the order of 24.5w/o.

(3) A four-phase ternary eutectic ($L \rightleftharpoons \beta + \theta + ZrFe_2$) occurs between 930° and 935°C.

(4) It is likely that a four-phase ternary peritectoid ($\beta + \theta \rightleftharpoons \alpha + ZrFe_2$) occurs at a temperature just above the binary zirconium-iron eutectoid (which takes place between 790° and 800°C). A four-phase ternary eutectoid ($\beta \rightleftharpoons \alpha + \theta + ZrFe_2$) taking place just above the zirconium-iron eutectoid remains an alternate possibility.

(5) The solubility limit of alpha-zirconium was found to be extremely low in the presence of iron, falling below the most dilute binary iron and ternary alloys prepared at 600°C and lower.

VI. CONTRIBUTING PERSONNEL AND LOGBOOKS

Data relating to the work reported herein are recorded in ARF Logbook C-5826.

The following personnel have contributed to the work:

J. J. Brophy	Magnetic Susceptibility Data
W. A. Buknas	Heat Treatment
J. R. Dvorak	Metallography
D. W. Levinson	Supervisor
L. C. Malevitis	Arc Melting
M. E. Runner	Chemical Analysis
R. E. Steiner	Arc Melting
B. J. Stang	Metallography
L. E. Tanner	Project Leader
M. Wright	Project Technician

Respectfully submitted,

ARMOUR RESEARCH FOUNDATION
OF ILLINOIS INSTITUTE OF TECHNOLOGY

Lee E. Tanner

L. E. Tanner
Associate Metallurgist

David W. Levinson

David W. Levinson
Assistant Manager
Metals Research

REFERENCES

1. Tanner, L. E. and D. W. Levinson, "The System Zirconium-Iron-Tin," Summary Report ARF-2068-4, Contract No. AT(11-1)-315 (Aug. 12, 1957).

2. Hansen, M., H. D. Kessler and D. J. McPherson, "The Titanium-Silicon System," Trans. ASM 44 (1952), 518.

3. Dupraw, W. A., "Determination of Tin in Titanium Alloys," Analytical Chemistry 26 (Oct. 1954), 1642.

4. Bates, L. F., Modern Magnetism (Cambridge University Press, London, 1951), 122.

5. Hayes, E. T., A. H. Roberson and W. L. O'Brien, "Constitutional and Mechanical Properties of Zirconium-Iron Alloys," Trans. ASM 43 (1951), 888.

6. Goodwin, J. G., J. D. Grozien, L. S. Rubinstein and F. L. Shubert, "A Postulation on the Source of Stringer Corrosion of Zircaloy-2," Zirconium Highlights, WAPD-ZH-3 (Jan. 1958) 5.

7. McPherson, D. J. and M. Hansen, "The System Zirconium-Tin," Trans. ASM 45 (1953), 915.

8. Elliott, R., private communication.

9. Selwood, P. W., Magnetochemistry, 2nd Ed. (Interscience Publishers, New York, 1956), 363.